Smart usage of context information for the analysis, design and generation of power-aware policies for mobile sensing apps

Rafael Pérez Torres

Dr. César Torres Huitzil
Dr. Hiram Galeana Zapién

Doctoral seminar, 2017

Structure

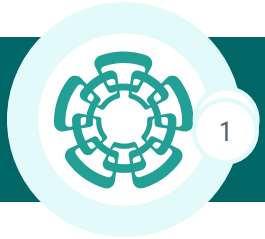

Research background
Motivation

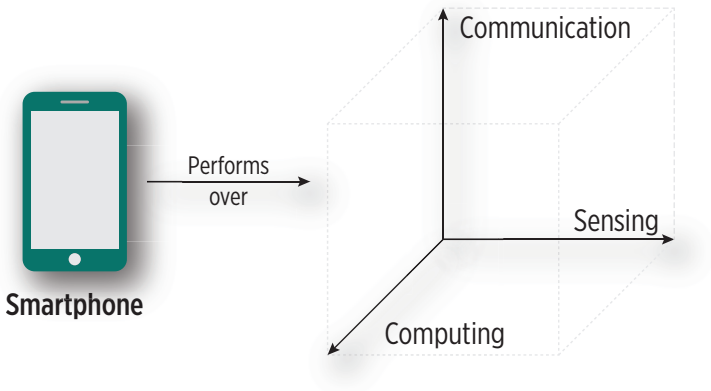

Figure: The advances in the communication, computing and sensing dimensions of mobile devices contribute to their acceptance by society.

Motivation

- The sensing dimension enables *context-awareness* in mobile devices, such as the smartphone.
  - ~~**Context** is the set of environmental states and settings that determines an application's behavior [1].~~
- Battery advances are slower than those of other smartphone components [2], growing 5-10% yearly [3, 4].
  - The energy constraint is critical when continuous access to sensors is needed, which is a core requirement of **mobile sensing applications**.

Research background
Motivation

Motivation

- For the sensing dimension, scientific efforts have been done for achieving the energy efficiency of the GPS location provider.
- The understanding of mobility could augment the location-awareness of the smartphone for many purposes, such as energy savings and the development of Mobility Based Services (MBSs).
- As a high level of abstraction, mobility can be characterized as a sequence of frequently visited places (a.k.a. stay points).

Research background
Problem statement

- The understanding of mobility is possible at different spatial-temporal scales:

Fine-grain mobility patterns identification

- They refer to the transportation mode employed by user when moving between stay points.
- Given a set of values $\mathcal{V} = v_{acc\ 1}, v_{acc\ 2}, \ldots, v_{acc\ n}$ obtained from accelerometer in the time interval $[t_1, t_2]$, identify fine-grain mobility information:

$$\textbf{FineGrainMobilityIdentifier}(\mathcal{V}) \rightarrow p_S \in \{\text{static, walking, biking, vehicle}\}$$

with each $v_{acc\ i} \in \mathcal{V}$ composed as $\langle acc_x, acc_y, acc_z, t \rangle$.

Coarse-grain mobility patterns identification

- They refer to motion at a large spatial scale related to user visiting stay points.
- Given a set of values $\mathcal{V} = v_{gps\ 1}, v_{gps\ 2}, \ldots, v_{gps\ n}$ obtained from GPS location provider in time interval $[t_1, t_2]$, identify coarse-grain mobility information:

$$\textbf{CoarseGrainMobilityIdentifier}(\mathcal{V}) \rightarrow p_S \in \{\text{new stay point, arrival, departure}\}$$

with each $v_{gps\ i} \in \mathcal{V}$ composed ~~associated~~ $\langle lat, lon, t \rangle$.

Research background
Problem statement

Sensors sampling adaptation

- Given a set of coarse and fine-grain mobility patterns $\mathcal{P} = \{p_{s_1}, p_{s_2}, \ldots, p_{s_n}\}$, and accuracy requirements of mobile app $req_{accuracy}$, implement a sampling policy for the adaptive duty cycling of sensors while reducing energy consumption:

$$\textbf{PolicyGeneration}(\mathcal{P}, req_{accuracy}) \longrightarrow \mathcal{S}_{conf}$$

where $\mathcal{S}_{conf} \rightarrow s, \mathcal{T}_{real}$ represents the sampling $\mathcal{T}_{real}$ that must be implemented for sensor s. The $req_{accuracy}$ refers to the granularity of GPS sampling.

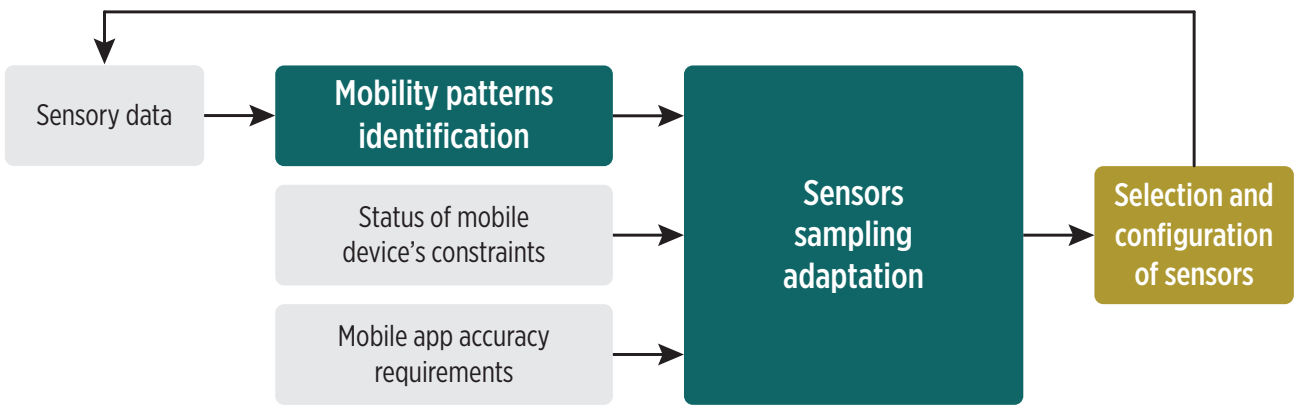

Figure: Interaction between problems.

Research background
Hypothesis

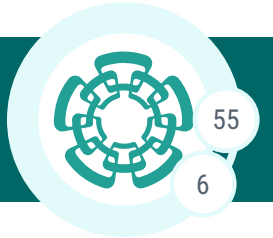

Hypothesis

- The energy consumption of continuous and extended location tracking could be reduced by means of a cognitive dynamic system that learns an expanded spatial-time model from mobility events detected from sensors data and that employs such model in a cognitive controller for dynamically adapting GPS sampling rate through sampling policies tailored to current mobility state.

Research background
Objectives

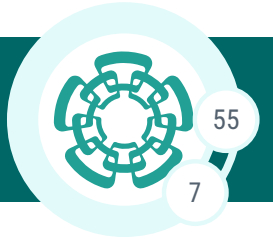

Main objective

- To reduce the energy consumption of mobile sensing apps, which perform continuous sensor sampling, through self-adapting power-aware policies generated from context information obtained from sensors data.

Particular objectives

- To detect mobility patterns from context information obtained from an inertial sensor (accelerometer) and location provider (GPS).
- To generate an accurate representation of detected patterns for summarizing user mobility.
- To dynamically adapt GPS sampling rate by means of a cognitive controller that employs the learned mobility representation and accuracy requirements for implementing power-aware sampling policies.
- To ease the development of mobile sensing applications that require user location tracking, i.e., LBSs and MBSs, isolating the complexity of sensors access and the associated efficient energy management.

Research background
Contributions

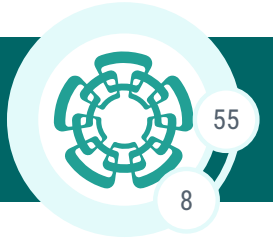

Contributions

- An on-device mobility patterns detector that works with streams of raw data collected by smartphone's sensors (GPS and accelerometer).
- An on-device mobility analyzer that incrementally builds a model of user mobility from the detected mobility patterns.
- A cognitive controller inspired on CDSs that, based on the mobility information learned, dynamically adapts GPS sampling rate through power-aware policies.
- A middleware with the previous modules embedded for easing the development of LBSs and MBSs for the Android mobile platform.

Research background
Methodology

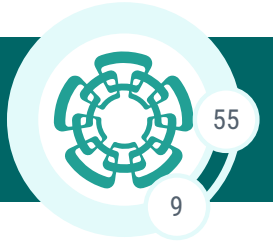

Methodology

1. Revision of state of the art power-aware sensing techniques.
2. Formal definition and selection of mobility patterns to be identified.
3. Research on algorithms for detecting mobility patterns.
4. Design of the *Mobility Events Detector*.
5. Design of adaptive policies for energy efficient usage of sensors.
6. Design of the Cognitive Controller.
7. Development of a middleware involving the *Mobility Events Detector* and the Cognitive Controller for the Android platform.
8. Experimentation in terms of spatial-time accuracy and energy efficiency.

State of the art
Mobile Sensing Apps (MSAs)

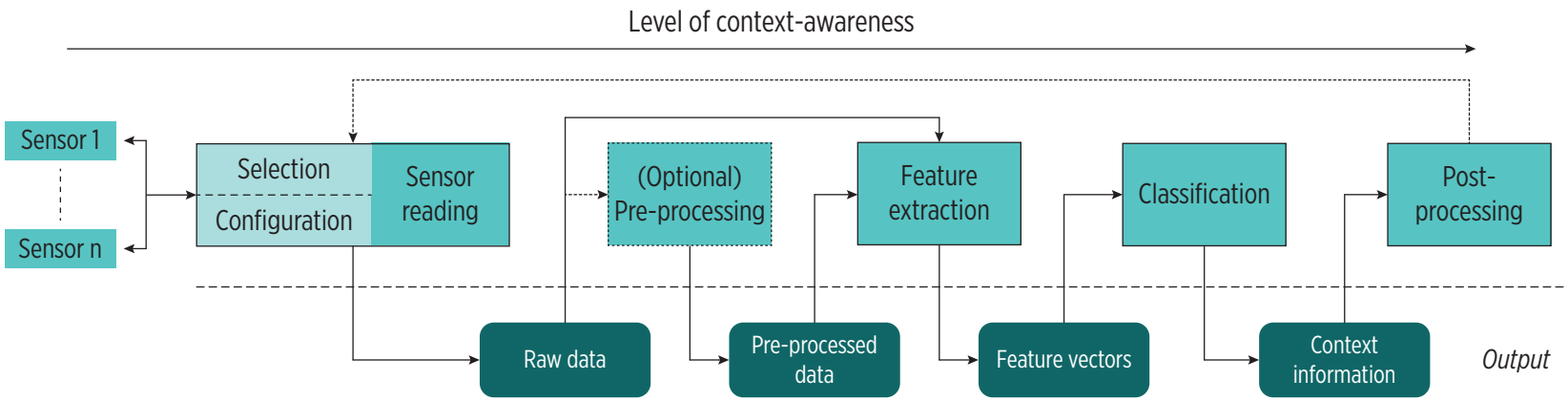

Figure: Stages of mobile sensing apps.

State of the art
Taxonomy of solutions

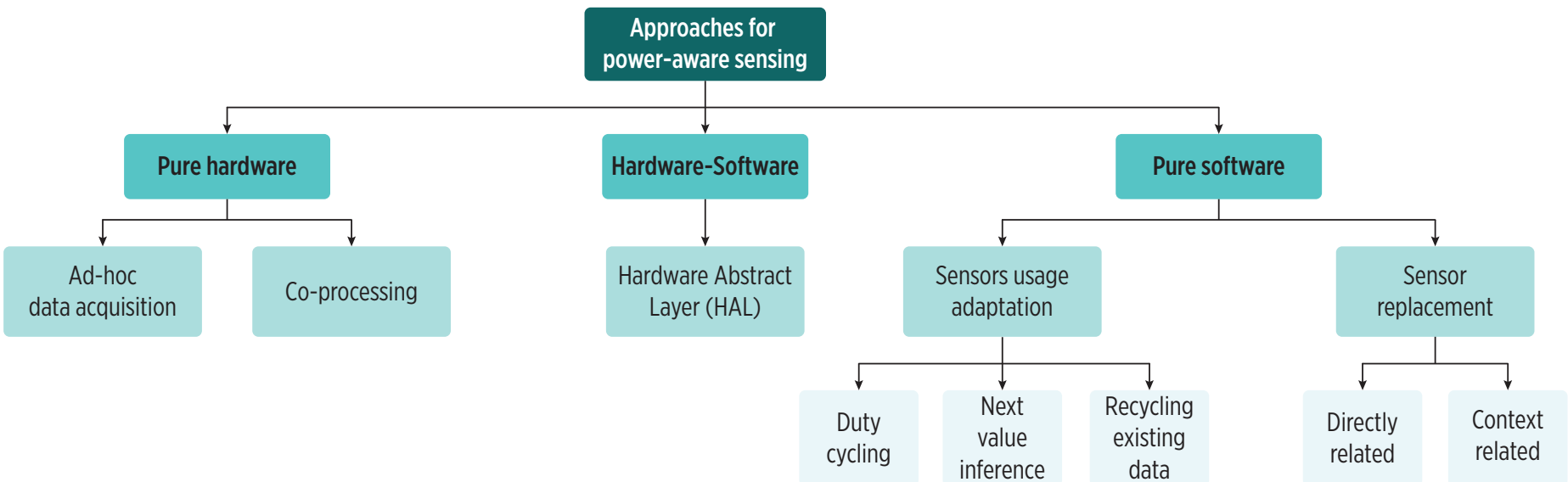

Figure: Taxonomy of solutions for power-aware sensing in mobility sensing systems.

State of the art
Remarks

Remarks

- The exploitation of coarse and fine-grain mobility information for modeling and characterizing user mobility has been barely explored.
- Although some of the proposed solutions employ a duty cycling strategy, it is fixed and obeys to instant mobility information, neglecting the temporal evolution of user mobility.
- A spatial-time accurate and energy efficient adaptive sampling could be produced by a cognitive approach that understands long-term mobility from fine and coarse-grain mobility events.
- The cognitive approach goes beyond typical pattern recognition and classic control strategies that follow a static configuration, as it evolves (in the learning and action tasks) across time.
- The smartphone itself could augment not only its location but also its mobility awareness (per-user basis).

Theoretical framework

Stay points

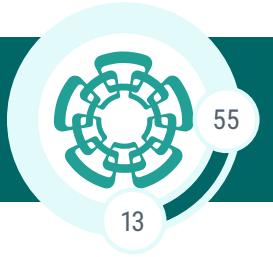

Definition

- A stay point refers to a geographical zone where the user remains for an amount of time.
- It is a virtual location defined by latitude (*lat*), longitude (*lon*), arrival time (*at*) and departure time (*dt*).

Calculation

- A GPS position fix p is defined by latitude (*lat*), longitude (*lon*), and timestamp (t).
- A stay point (**sp**) is calculated from a set of consecutive GPS fixes $\mathbf{P} = \{p_m, p_{m+1}, \ldots, p_n\}$, and $\delta_{distance}$ and δ_{time} thresholds.
- Its composition must observe:

$$|p_n.t - p_m.t| \geq \delta_{time} \qquad \text{distance}(p_m, p_i) \leq \delta_{distance}, \forall m < i \leq n$$

- Its centroid coordinates are the arithmetical means:

$$\mathbf{sp}.lat = \frac{\sum_{i=m}^{n} p_i.lat}{|\mathbf{P}|} \qquad \mathbf{sp}.lon = \frac{\sum_{i=m}^{n} p_i.lon}{|\mathbf{P}|}$$

- The *at* and *dt* components are set to $p_m.t$ and $p_n.t$, respectively.

Theoretical framework

Event Driven Systems (EDSs)

Event

- It is an occurrence within a particular system-domain [5] at an specific timestamp or during a time interval.
- Formally defined as:

$$ev = ev(id, \{a_1, a_2, \ldots, a_n\}, t)$$

where *id* is an identifier, $\{a_1, a_2, \ldots, a_n\}$ is a list of *n* associated attributes, and *t* the timestamp.

Event Driven System (EDS)

- An EDS is a system that works by sending asynchronous event notifications between its components for triggering computing tasks [6, 5].
- Its complexity and coupling is reduced and it is power-aware by design (vs. synchronous systems [7, 8, 9]).

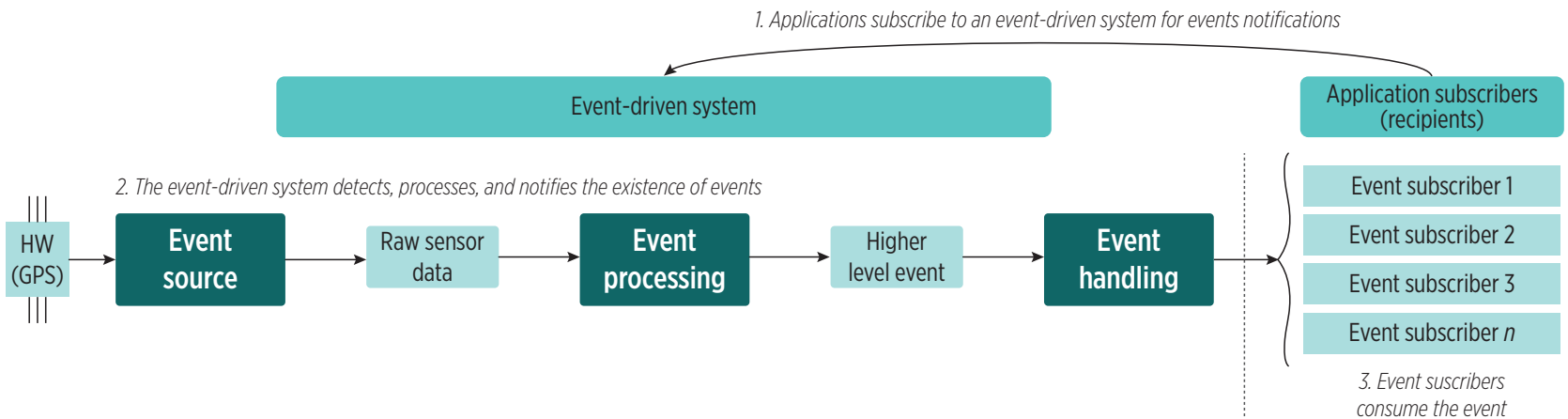

Figure: The architecture of an EDS.

Theoretical framework

Cognitive Dynamic Systems (CDSs)

Features

- Perception-action cycle
- Memory
- Attention
- Intelligence

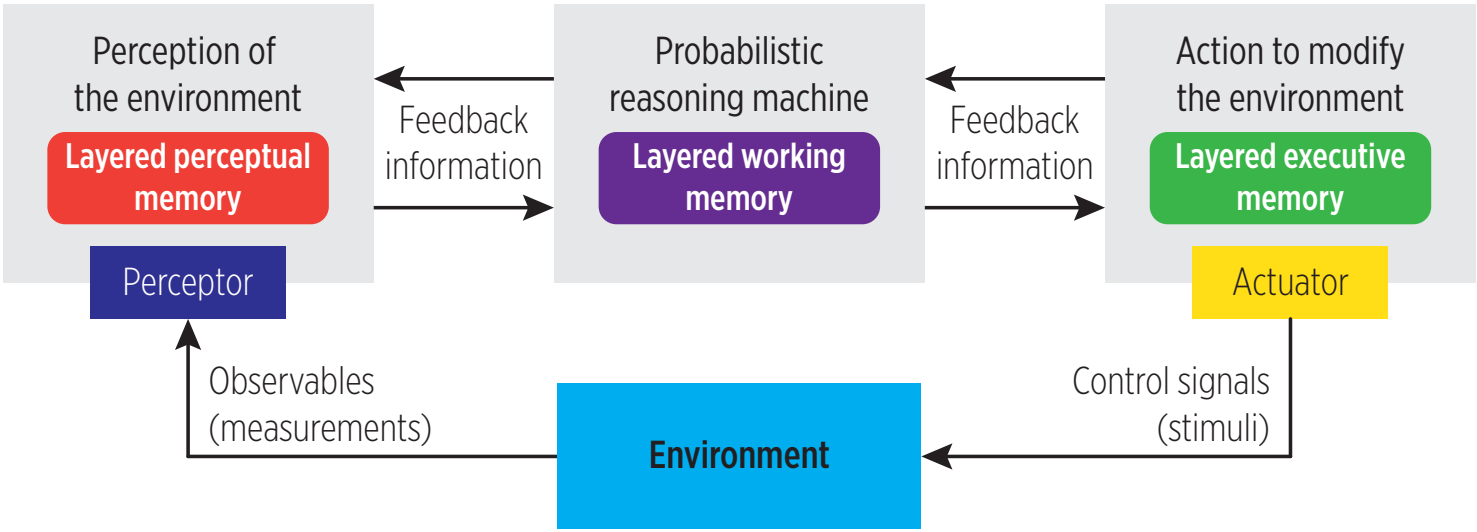

Figure: The generic architecture of a CDS.

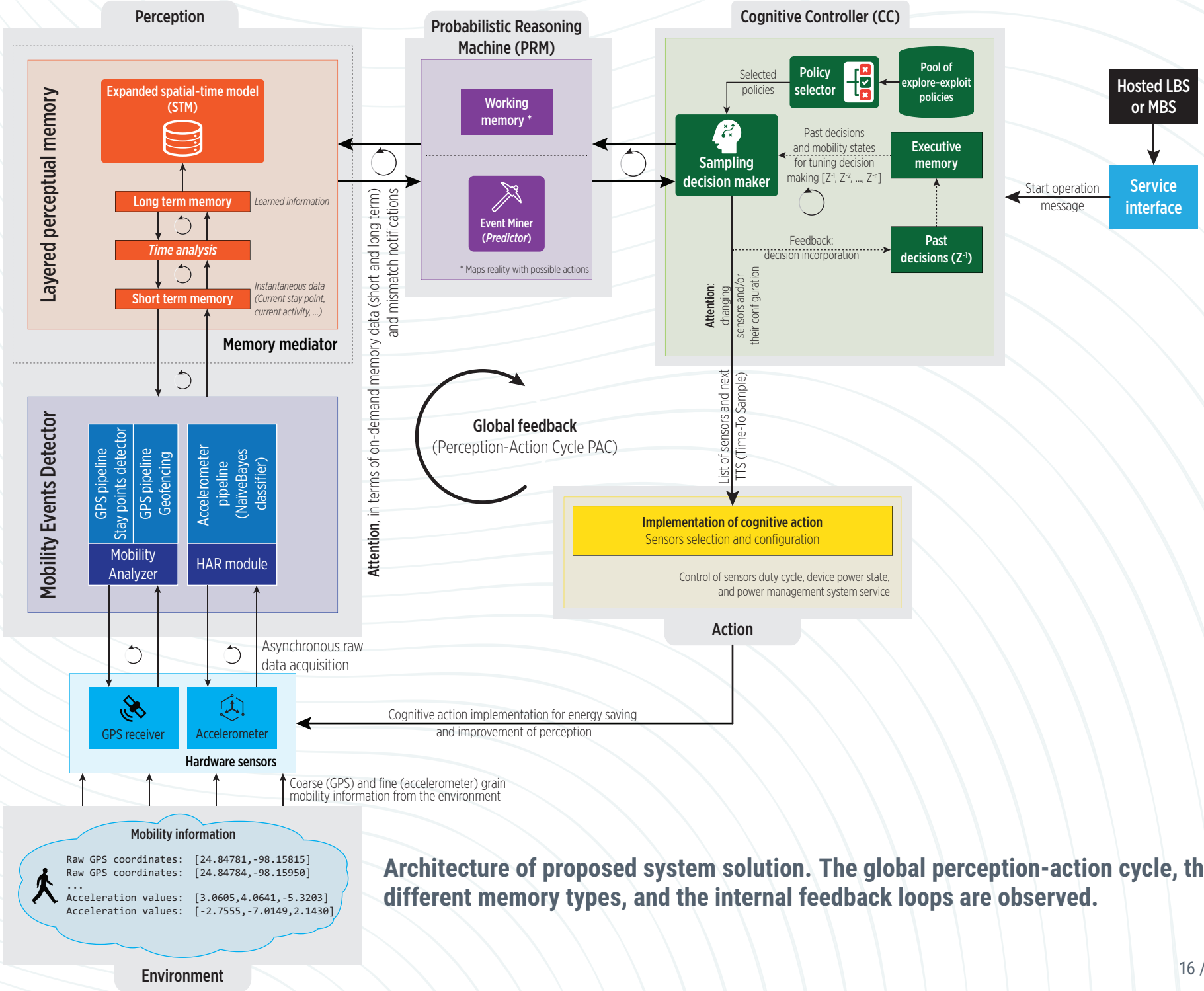

Architecture of proposed system solution. The global perception-action cycle, the different memory types, and the internal feedback loops are observed.

Perception components
Mobility Events Detector

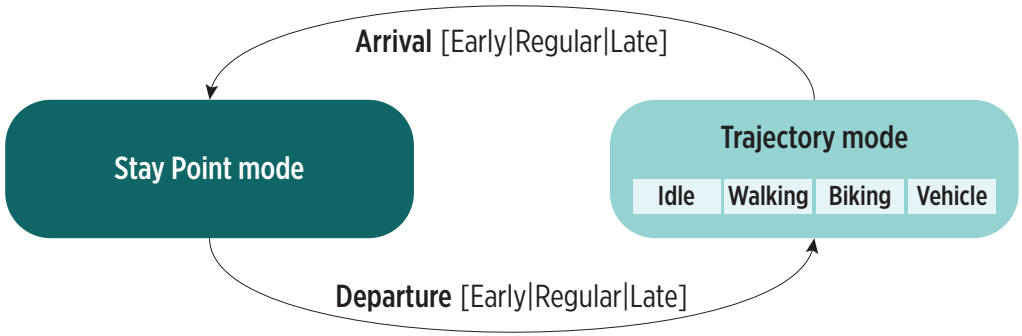

Figure: Individual's mobility as a sequence of high level states and associated events detected from raw sensor data [10, 11].

Mobility Events Detector

~~Perception components in the Mobility Events Detector tailored for identifying:~~

- Coarse-grain mobility events.
- Fine-grain mobility events.

Perception components

Mobility Events Detector: *Stay Points Detector* module

Stay Points Detector module

- Focused on detecting stay points in user mobility.
- Event-driven design, it incrementally processes each low-level mobility event (raw GPS data).

Stream of location updates (gs)

	Latitude	Longitude	Time
fix_1:	lat_1,	lon_1,	t_1
fix_2:	lat_2,	lon_2,	t_2
fix_3:	lat_3,	lon_3,	t_3
...	...	...	...
fix_n:	lat_n,	lon_n,	t_n
...	...	...	...

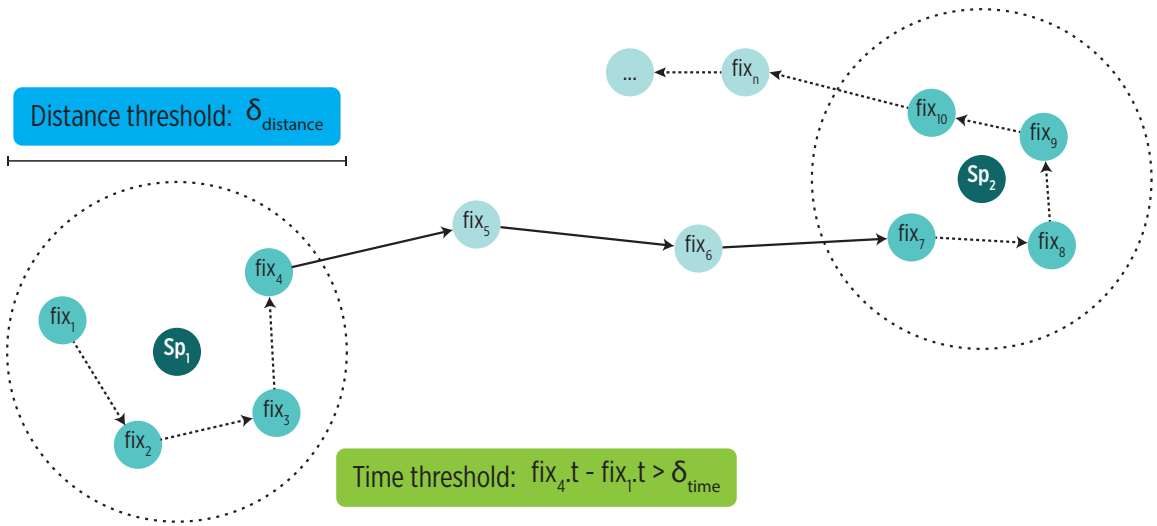

Figure: A conceptual representation of the stay points detection algorithm behavior.

Perception components

Mobility Events Detector: *Geofencing* module

Geofencing module

- Window-based approach with voting system.
- Requires an $SPS_{candidate}$ list of stay points.
- Incrementally analyzes location fixes for detecting coarse-grain mobility events under a $gf_{distance}$ threshold:

Older fixes window	Pivot (gf_{pv})	Newer fixes window	Outcome
outside	inside	inside	$arrival = (sp, t_{in})$
inside	outside	outside	$departure = (sp, t_{out})$
inside	inside	inside	$no\_change_{sp} = (sp, t)$
outside	outside	outside	$no\_change_{trj} = (none, t)$

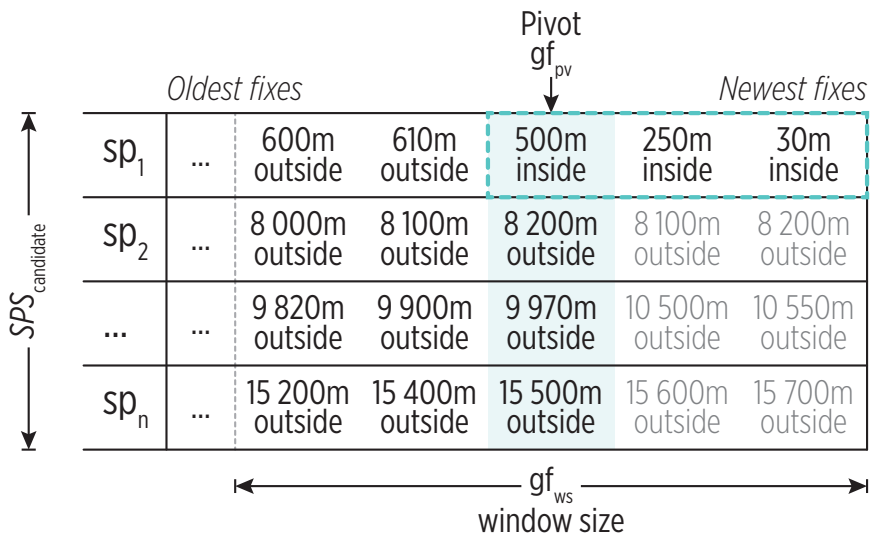

Figure: A conceptual representation of the window-based geofencing operation.

Perception components

Mobility Events Detector: *HAR* module

HAR module

- Window-based approach.
- Detects transportation mode from accelerometer data.
- Underlying NaïveBayes classifier.

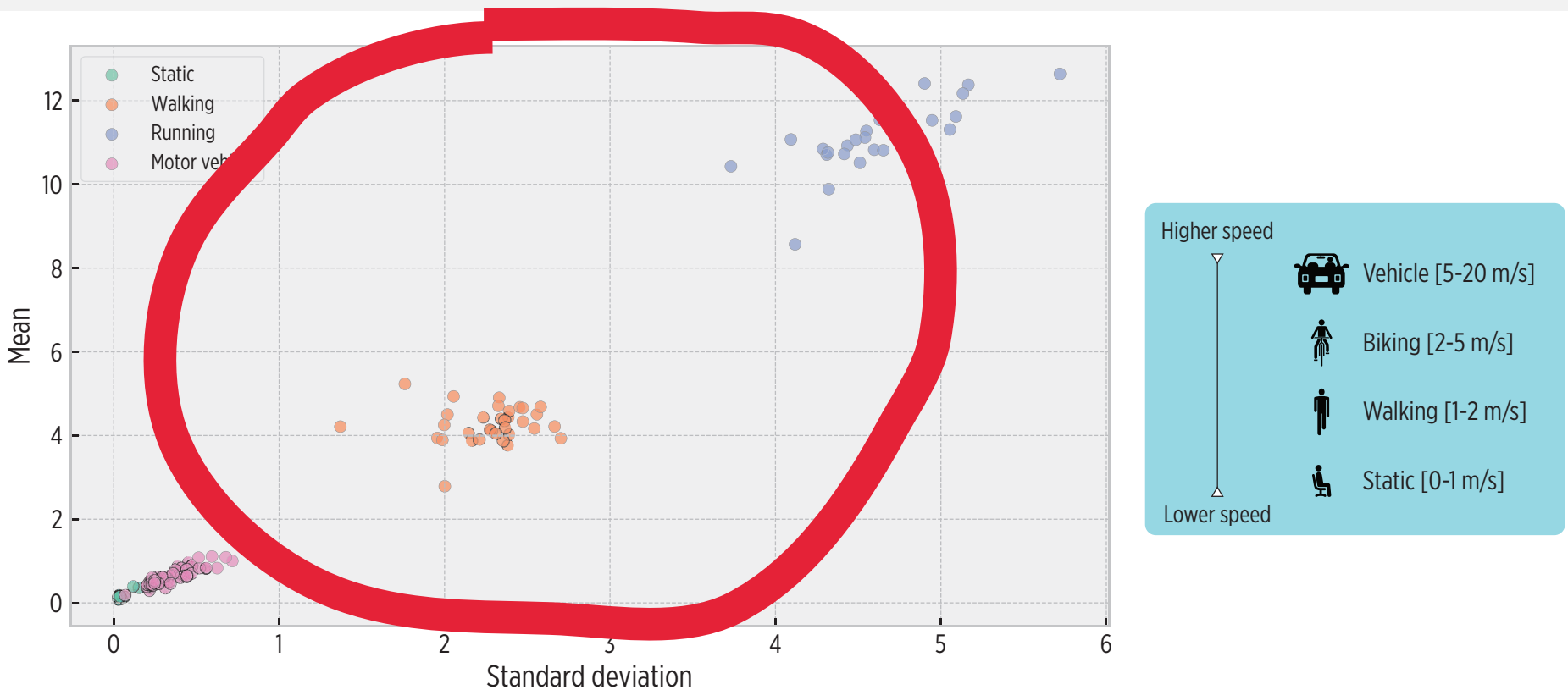

Figure: Distribution of mean and standard deviation features employed by the NaïveBayes classifier of the HAR module.

Layered perceptual memory

Short and long-term memory information

Layered perceptual memory

- Short-term memory information: current (observed) mobility status.
- Long-term memory information: the Expanded Spatial-Time model (STM).

Expanded Spatial-Time model

- The highest level of mobility information held by the system.

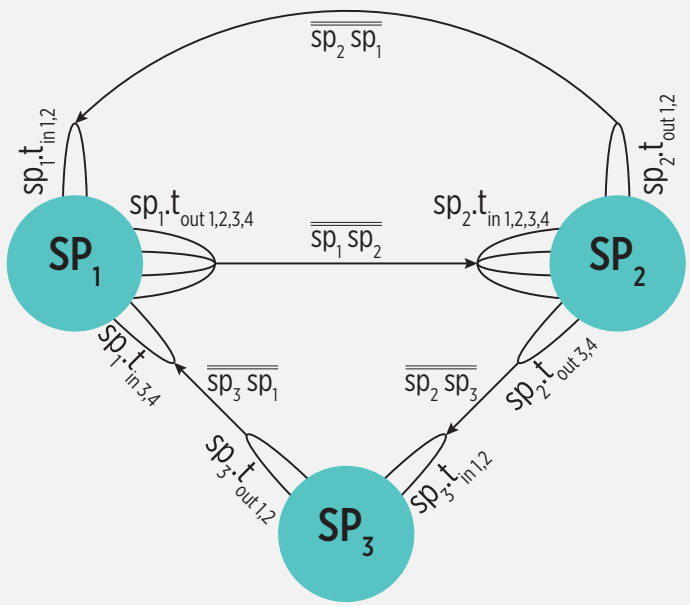

$\overline{sp_1\ sp_2}$ A summarized trajectory between sp_1 and sp_2
$\overline{sp_2\ sp_1}$ A summarized trajectory between sp_2 and sp_1
$\overline{sp_2\ sp_3}$ A summarized trajectory between sp_2 and sp_3
$\overline{sp_3\ sp_1}$ A summarized trajectory between sp_3 and sp_1

Figure: A conceptual representation of the STM's structure.

Layered perceptual memory

Expanded Spatial-Time model (STM)

Generation of the STM

- Incrementally built with the coarse-grain mobility events detected by the *Mobility Events Detector*.

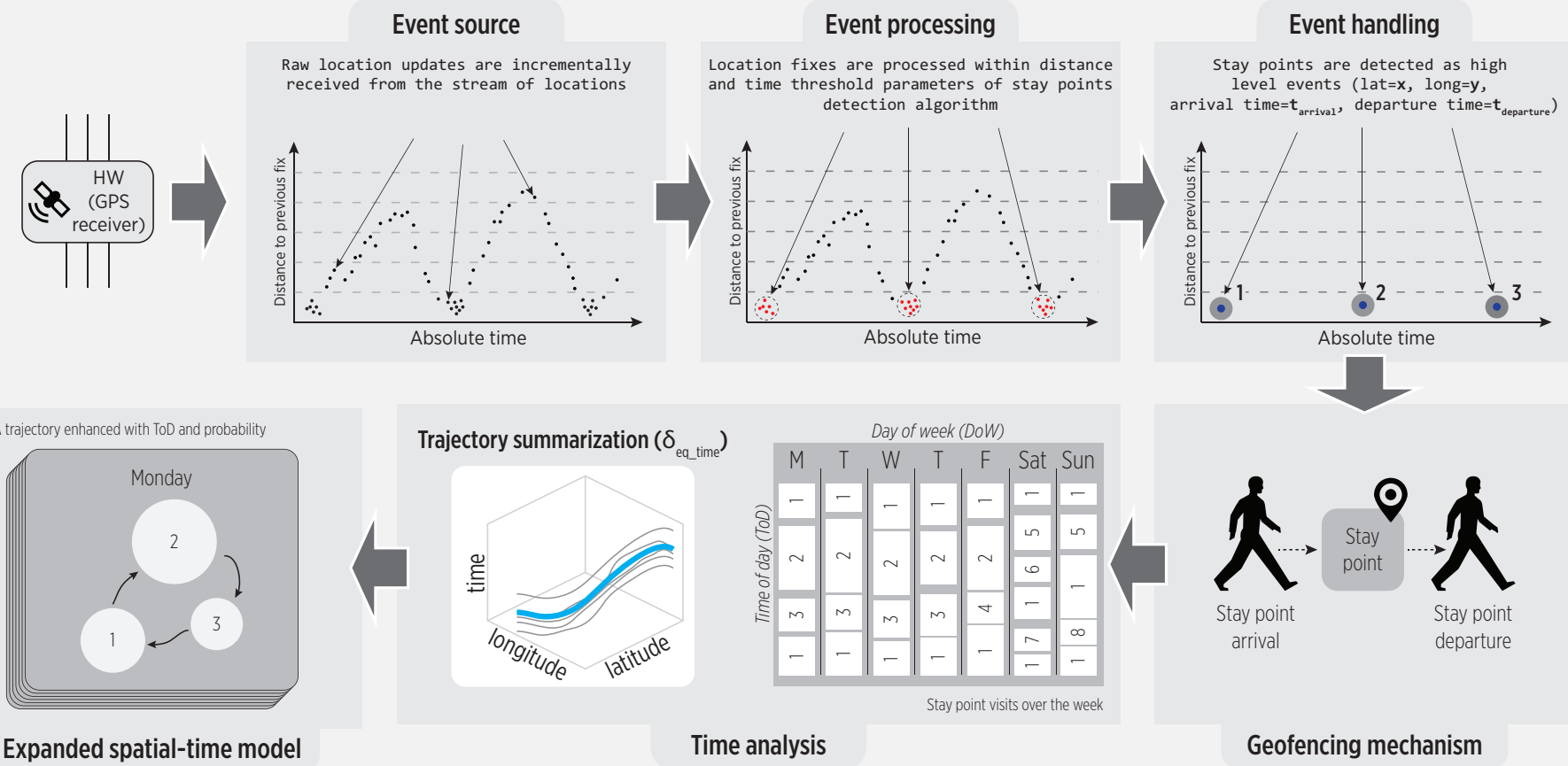

Figure: A conceptual representation of the steps for generating the STM from raw sensors data.

Working memory

Probabilistic Reasoning Machine (PRM)

PRM features

- It gives a meaning to the observed mobility information with respect of the STM information.
- It produces an estimation of future mobility state that links perceptual and working memory.

Interpretation

- The *Event Miner* traverses the STM for identifying whether learned information is:
  - Consistent, or
  - Inconsistent (mismatch)

  with respect of observed mobility information.

Estimation

- The *Event Miner* looks in the STM for a link (if any) with learned mobility information for generating spatial-time estimations:
  - Get next departure time.
  - Get next arrival time.

Cognitive controller (CC)

Description

Goals

- To reduce the energy consumption of location tracking by relying on PRM's estimations.
- To reduce the system uncertainty about current user mobility.

Possible cognitive actions

- **Exploitation policies**: When system uncertainty is low for saving energy purposes.
- **Exploration policies**: When system uncertainty is high for recovering for accuracy loss.

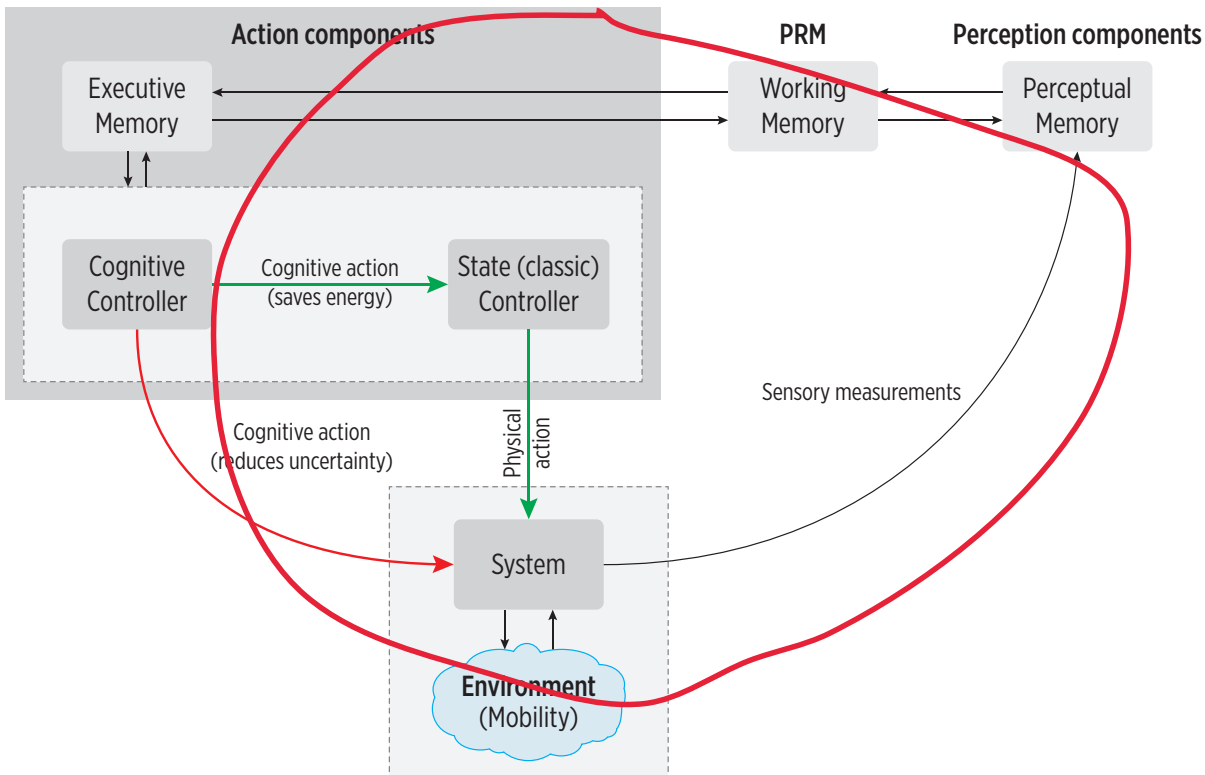

Figure: A cognitive controller generic architecture

Cognitive controller

Policies tailored for user mobility

Stay point mode

- A sampling based on the sigmoid function $sig(x) = \frac{1}{1+e^{-\alpha x}}$ as a model for the mobility phase transitions.
- Higher sampling rate on arrival and departure, when the user is more likely to move, and slower at the middle of a visit.

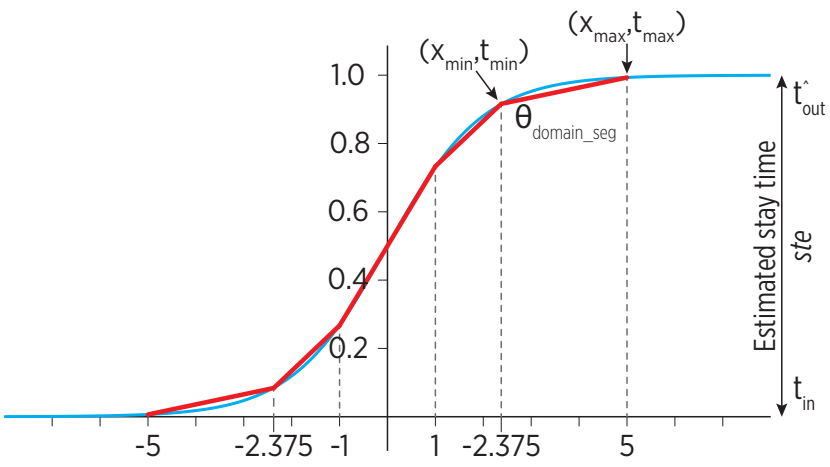

Figure: Approximation of the sigmoid through straight segments.

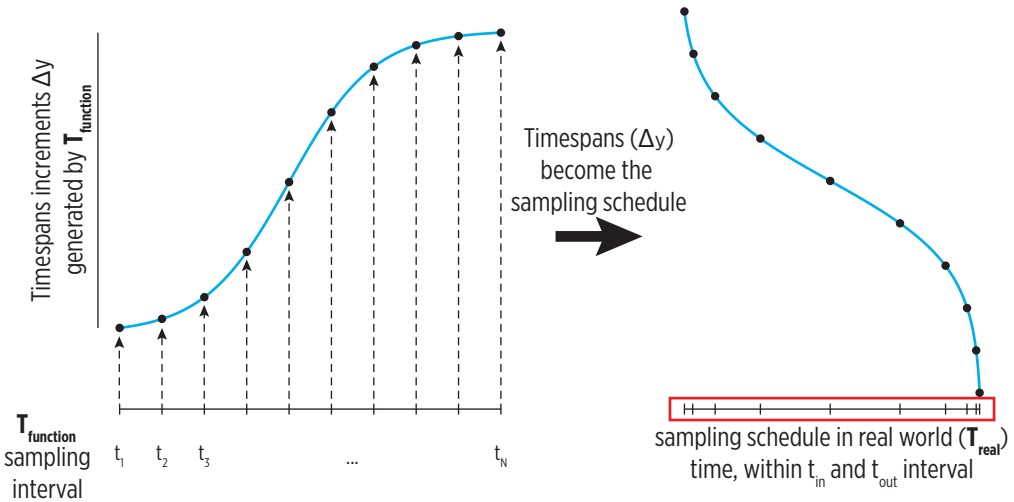

Figure: A snapshot of the process for producing a sigmoid sampling.

Cognitive controller

Policies tailored for user mobility

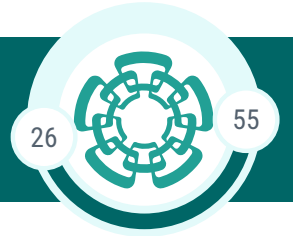

Trajectory mode

- The spatiotemporal characterization of people's motion during trajectory is complex: it is hard to produce a single spatiotemporal model for summarizing how all people move.
- No special modeling of motion during a trajectory is performed other than the user moves within a speed range.
- A hint of such speed is provided by the HAR module from the detected transportation mode.

Cognitive controller
Sampling Decision Maker module

Sampling Decision Maker module

- It filters from the *pool of exploration-exploitation policies* those apt for the mobility state detected by PRM.
- It implements one policy, employing the spatial-time estimation provided by the PRM.
- It updates its *Executive Memory* with the selected cognitive action for feedback in further executions.

Reaction for mobility events

- Reaction for arrival event:
  - The sampling rate is reduced by following a sigmoid-based sampling.
- Reaction for departure event:
  - The sampling rate is increased by implementing a target sampling T_{target}.

Cognitive controller
Mobility mismatches

Mismatches

- A mismatch represents a discrepancy between observed and learned mobility information.
- In general, the system increases the sampling rate for recovering the accuracy lost.

Reaction for mobility mismatches

- Reaction for early arrival:
  - The sampling rate is reduced by following a sigmoid-based sampling.
- Reaction for early departure:
  - The fastest sampling rate is selected for recovering accuracy and improving system perception.
- Reaction for late arrival:
  - The fast sampling rate must be maintained as long as the user is still in trajectory.
- Reaction for late departure:
  - A *conservative sampling* rate is implemented for detecting the eventual departure.

Attention and Intelligence

Distributed features

Attention

- Not all, but only the relevant mobility events are detected by perception components.
- The information learned by the STM is for characterizing user mobility and sampling rate adaptations.
- The system autonomously works towards detecting and learning such information.

Intelligence

- Manifested through the feedback loops within the system.
- Perception components and the sampling adaptation tasks are always aware of the current mobility state.
- Time is explicit for intelligence as the self-adaptiveness only makes sense across time when the spatial - time mobility is learned, or from a broader perspective, when changes are detected in the environment.
- If the role of time were not considered in the proposed system, only a static behavior based on instant mobility information would be achieved.

Implementation
Android device implementation

Smartphone device

The Google Nexus 6 smartphone with Android 7 was employed.

- Quad-core 2.7 GHz Krait 450 mobile processor (Qualcomm Snapdragon 805 chipset).
- 3 GB RAM.
- Qualcomm Snapdragon 805 chipset.
- 3220 mAh battery.

Technical barriers

1. Asynchronous access to sensors, affected by sensing infrastructure (GPS satellite signal intermittency).
2. Out-of-the-box energy saving mechanisms:
   - Application specific: **App StandBy**.
   - System wide: **Doze mode**.

Workarounds

1. Grace periods for sampling (`Timer` + `TimerTasks`).
2. `Alarms`, `WakeLocks`, foreground services.

The architecture of the proposed system implemented in the Android software stack.

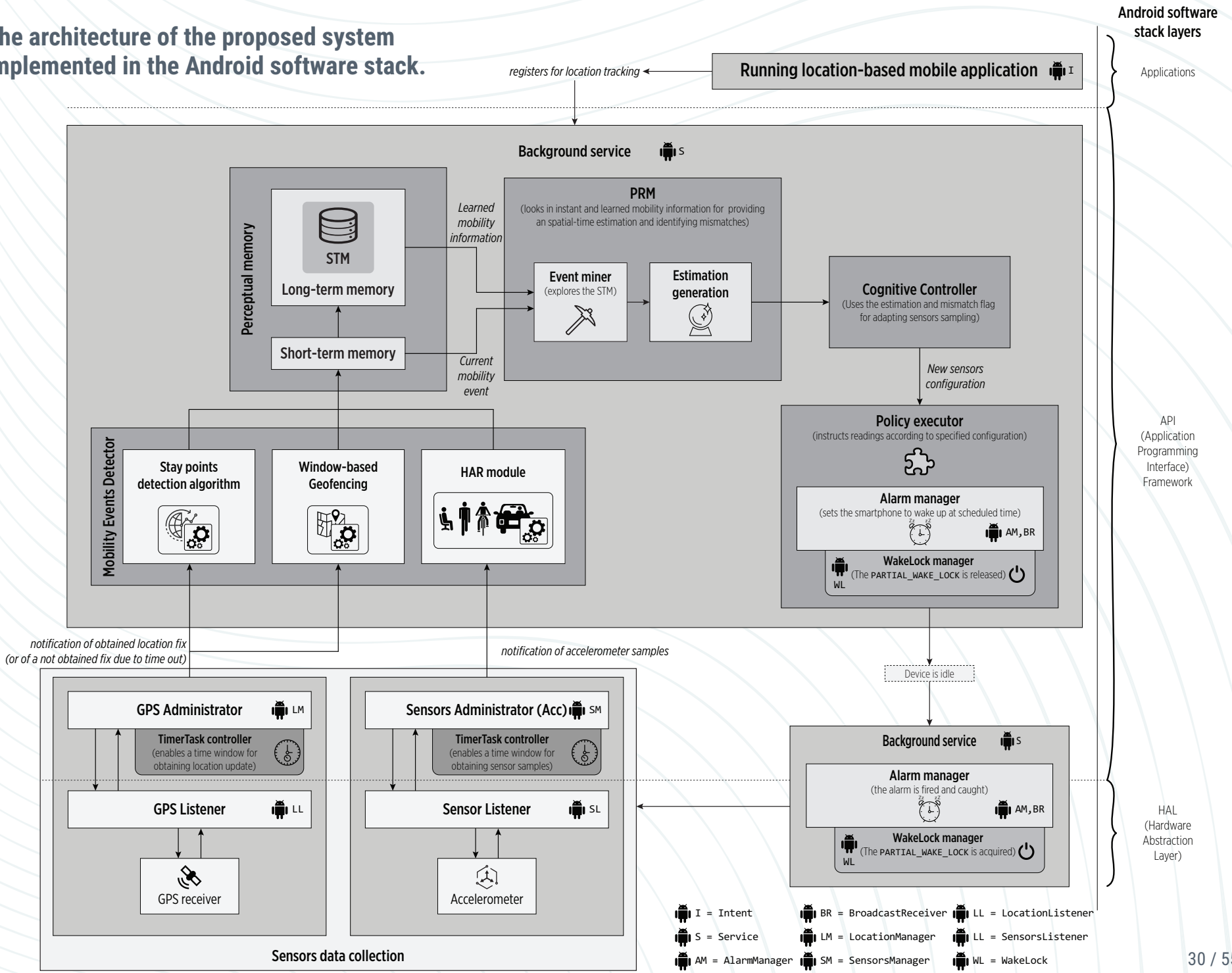

Preliminary experimentation
Materials and methods

Attributes evaluated

- Spatial-time accuracy.
- Energy consumption.

Desktop version

- It features different modules of the proposed system (except from HAR module).
- It allows the quick evaluation of system performance through different parameter combinations.
- It includes a logic *trajectory file* reader that simulates user motion.

On-device trials

- Two Nexus 6 smartphone units.
- The smartphones were always carried together with the GPS logger device by a campus student.
- No mobile apps other than the developed middleware were executed by the smartphones.
- The smartphones were not employed for communication tasks (texting, calls).

Preliminary experimentation

Materials and methods

Ground-truth mobility information

- High frequency (1 *Hz*) location data collected employing a Qstarz BT-Q1000eX GPS logger.
- 6 trajectories collected by the same user, mostly using a vehicle as transportation mode.

Stay Points Detector	**Time threshold** (δ_{time}):	45 *min*
	Distance threshold ($\delta_{distance}$):	500 *m*
Geofencing	**Radio distance** ($gf_{distance}$):	250 *m*
	Window size (gf_{ws}):	3
Sampling period:	1 second	

Table: Input parameters for the discovery of ground truth mobility information.

Trajectory	Duration (days)	Inside SP time (minutes)	In traj. time (minutes)	Total SPs	Total visits	Individual SP weight	
Trajectory 1	5.38	7,442.10 (96.06%)	305.07 (3.94%)	4	13	Home: 72.25% Bob's place: 0.94%	Cinvestav: 26.03% Store: 0.78%
Trajectory 2	6.05	8,348.42 (95.80%)	365.73 (4.20%)	6	21	Home: 69.67% Bob's place: 1.20% Store: 0.82%	Cinvestav: 26.51% Park: 0.99% Stadium: 0.82%
Trajectory 3	6.15	8,542.12 (96.53%)	307.45 (3.47%)	6	31	Home: 67.94% Park: 2.94% Fast food: 1.15%	Cinvestav: 24.50% Bob's place: 2.58% City center: 0.89%
Trajectory 4	7.22	10,024.63 (96.42%)	371.98 (3.58%)	2	16	Home: 66.50%	Cinvestav: 33.50%
Trajectory 5	7.35	10,026.22 (94.74%)	556.20 (5.26%)	4	19	Home: 67.29% Cinema: 2.41%	Cinvestav: 29.33% City center: 0.97%
Trajectory 6	34.31	47,599.62 (96.34%)	1,807.52 (3.66%)	11	146	Home: 65.31% Home 2: 2.81% Bob's place: 0.37% Store: 0.35% Workshop: 0.20% Workshop 2: 0.11%	Cinvestav: 29.36% Fast food: 0.71% Restaurant: 0.36% City center: 0.30% Store 2: 0.12%

Table: Mobility information of collected ground truth trajectories (SP=stay point).

Preliminary experimentation

Stay Points Detector module spatial-time accuracy

Description

- This experiment evaluates the spatial-time accuracy of the *Stay Points Detector* module under different GPS sampling rates in terms of centroid distances and latencies.

Stay Points Detector	**Time threshold** (δ_{time}):	45 *min*
	Distance threshold ($\delta_{distance}$):	500 *m*
Sampling periods:	30, 60, 90, 120, 150, 180 seconds.	
Trajectories:	All ground truth trajectories.	

Table: Input parameters for the spatial-time accuracy of stay points experiment.

Results

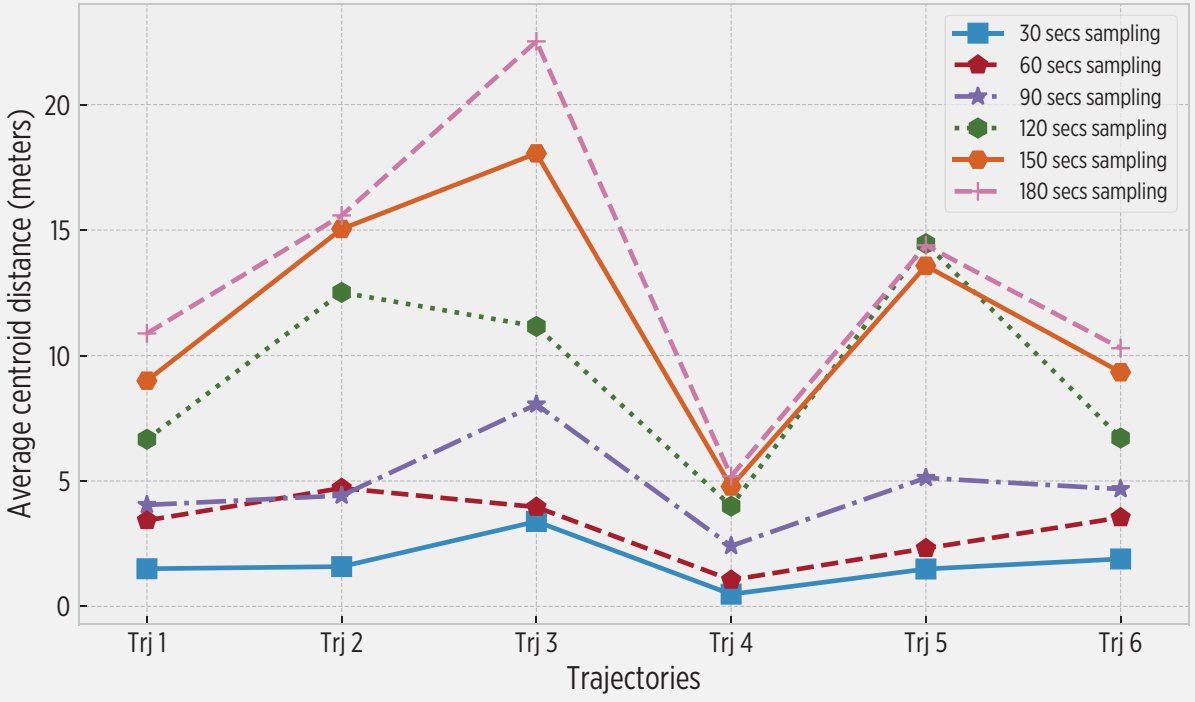

Figure: The impact of different sampling periods on the centroid distance of identified stay points in each trajectory. A maximum centroid distance of 22.52 *m* is identified when employing the 180 seconds sampling period.

Preliminary experimentation

Stay Points Detector module spatial-time accuracy: Results

Trajectory	Sampling period (seconds)	Live stay points identified	Average centroid distance (meters)	Average arrival latency (seconds)	Average departure latency(seconds)
Trajectory 1	30	12 of 12	1.50	2.67	24.92
	60	12 of 12	3.43	***-12.33***	17.42
	90	12 of 12	4.04	15.17	32.42
	120	12 of 12	6.66	***-7.33***	52.42
	150	12 of 12	9.00	25.17	79.92
	180	12 of 12	10.88	22.67	77.42
Trajectory 2	30	16 of 16	1.59	7.38	13.62
	60	16 of 16	4.72	20.50	34.25
	90	16 of 16	4.42	37.38	26.75
	120	16 of 16	12.51	16.75	83.00
	150	16 of 16	15.04	***-0.12***	96.12
	180	16 of 16	15.58	65.50	71.75
Trajectory 3	30	19 of 19	3.39	2.26	12.16
	60	19 of 19	3.96	11.74	12.16
	90	19 of 19	8.05	40.16	29.53
	120	19 of 19	11.16	37.00	56.37
	150	19 of 19	18.06	48.05	59.53
	180	19 of 19	**22.52**	87.53	81.63
Trajectory 4	30	13 of 13	0.49	16.15	2.46
	60	13 of 13	1.05	41.54	34.77
	90	13 of 13	2.41	32.31	55.54
	120	13 of 13	4.00	32.31	71.69
	150	13 of 13	4.78	41.54	50.92
	180	13 of 13	5.19	73.85	62.46
Trajectory 5	30	18 of 18	1.49	0.17	13.61
	60	18 of 18	2.31	13.50	21.94
	90	18 of 18	5.12	***-3.17***	23.61
	120	18 of 18	14.46	10.17	***-44.72***
	150	18 of 18	13.58	30.17	***-39.72***
	180	18 of 18	14.39	26.83	***-71.39***
Trajectory 6	30	75 of 75	1.89	2.89	6.89
	60	**76 of 75**	3.54	8.49	24.89
	90	**76 of 75**	4.67	7.29	59.69
	120	**76 of 75**	6.71	29.29	77.69
	150	75 of 75	9.33	42.89	113.29
	180	**76 of 75**	10.29	51.69	108.89

Table: Spatial-time differences in detected stay points per sampling period (ST=stay time). The negative values in the ST difference and the arrival and departure latencies

Preliminary experiments

Geofencing module spatial-time accuracy: Description

Description

- This experiment evaluates the spatial-time accuracy of the visits information detected by the *Geofencing* module under different GPS sampling rates, in terms of missed visits, and arrival and departure distance-latency.

Geofencing	**Radio distance** ($gf_{distance}$):	250 *m*
	Window size (gf_{ws}):	3, 5, 7
Sampling periods:	30, 60, 90, 120, 150, 180 seconds.	
Trajectories:	All ground truth trajectories.	
STM	Preloaded with corresponding ground truth stay points.	

Table: Input parameters for the spatial-time accuracy of Geofencing module experiment.

Preliminary experiments

Geofencing module spatial-time accuracy: Results

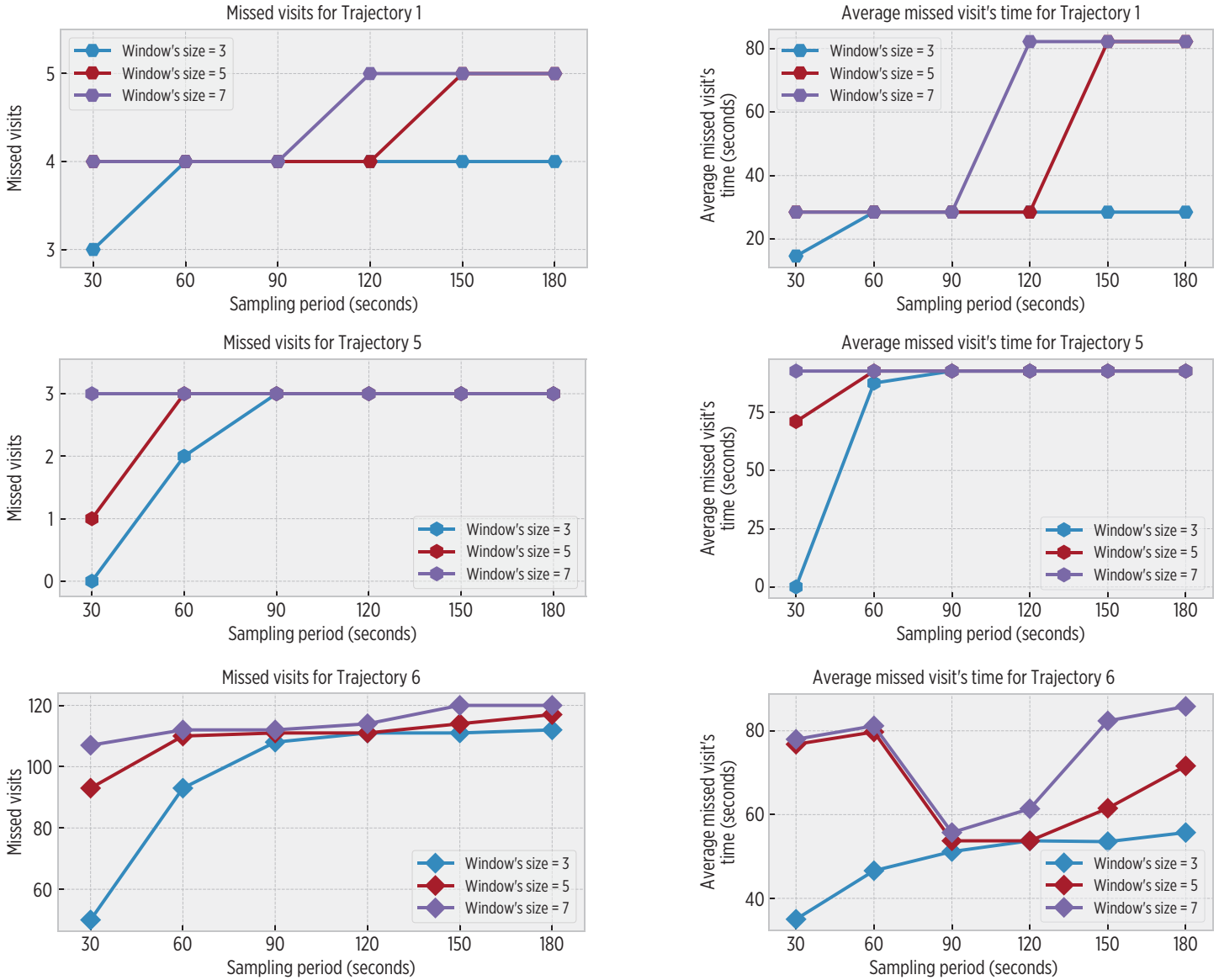

Figure: Visits missed by the *Geofencing* module for each combination of sampling period and window size values. The largest amount is obtained for the *Trajectory 6*, given its length (more than 30 days). Nevertheless, they do not account for a considerable time in overall trajectories.

Preliminary experiments

Geofencing module spatial-time accuracy: Results

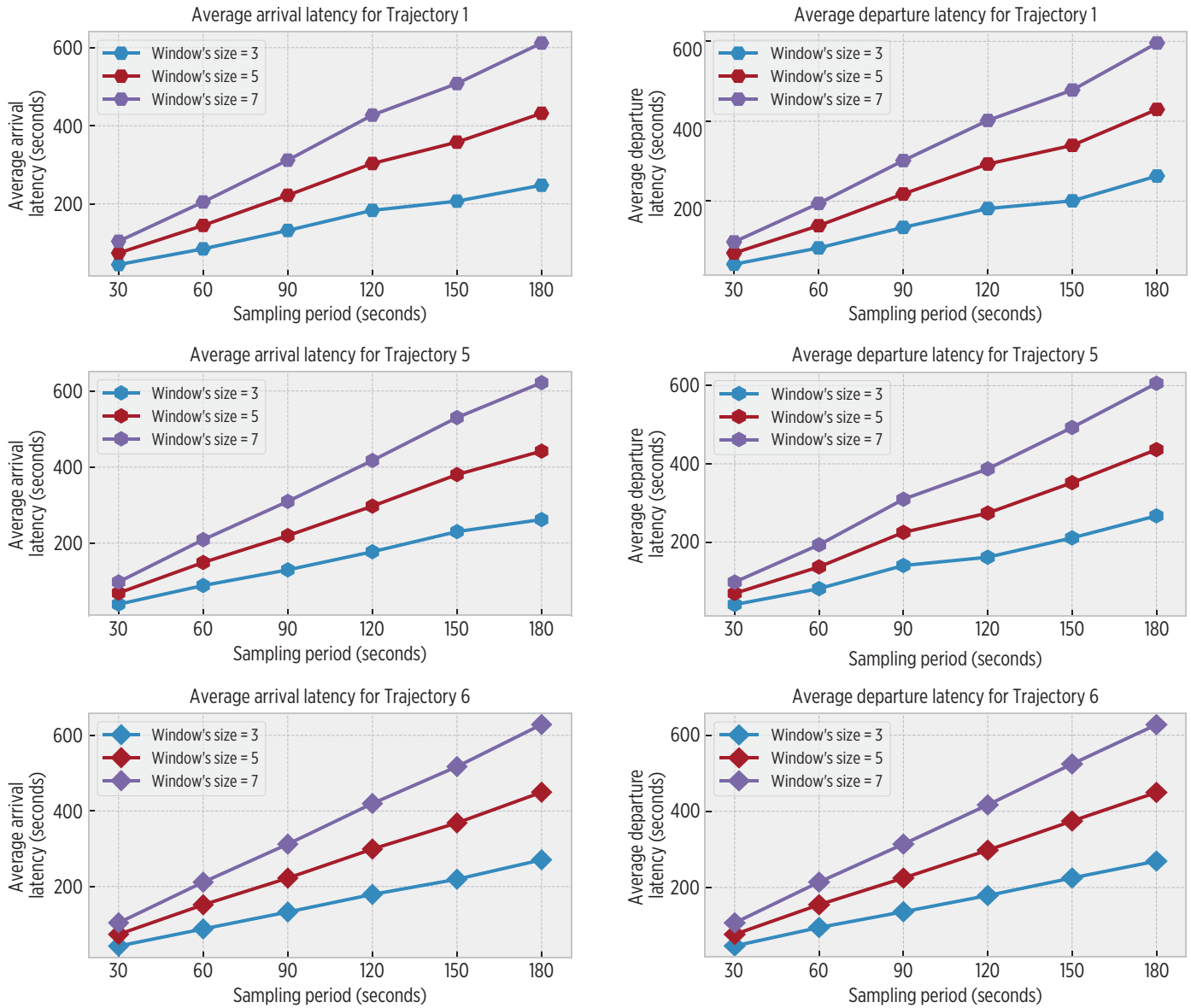

Figure: Arrival (left) and departure (right) latencies obtained by the Geofencing module for each combination of sampling period and window length values. There is a tendency on the results as the shortest window's sizes produce the shortest arrival latency values.

Preliminary experiments
Reaction to STM mobility mismatches: Description

Description

- This experiment was focused on evaluating the ability of the system for reacting to mismatches in mobility information, with a particular emphasis on mismatch departure events.
- For some trials the information of the STM was intentionally modified by giving it longer stay times than those in the actual visits.
- The missed visits, the delay for detecting the temporal mismatches, and the departure latency were evaluated.

Geofencing	**Radio distance** ($gf_{distance}$):	250 m
	Window size (gf_{ws}):	3
Cognitive Controller	**Sigmoid segments** (Θ_{domain_segs}):	$(-5, -2.375), (-2.375, -1), (-1, 1), (1, 2.375), (2.375, 5)$ $(-4, -2.375), (-2.375, -1), (-1, 1), (1, 2.375), (2.375, 5)$
	Time separations (Θ_{time_sep}):	$[90, 150, 180, 150, 90]$ seconds $[90, 120, 180, 120, 90]$ seconds $[60, 150, 180, 150, 60]$ seconds $[60, 120, 180, 120, 60]$ seconds
Trajectories	All ground truth trajectories.	
STM	Preloaded with ground truth stay points, with increased time (injured) in the proportions $[5, 10, 15, \ldots, 90, 95, 100]$ %	

Table: Input parameters for the reaction to mobility mismatches experiment.

Preliminary experiments

Reaction to STM mobility mismatches: Results

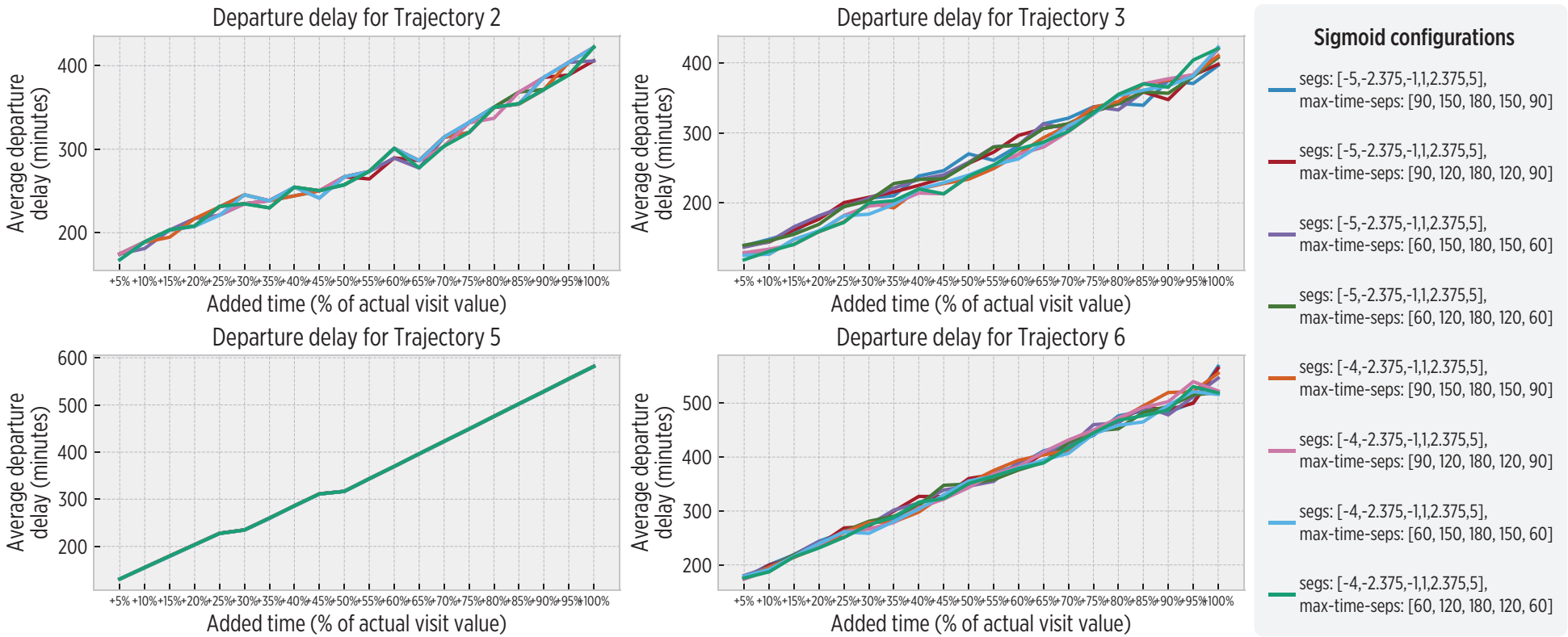

Figure: The evolution of the timespan between the expected and actual departures detected by the system across the different time increments applied to the STM. Similar tendencies are observed, highlighting that the sigmoid sampling allows to identify that user is leaving the stay points before expected.

Preliminary experiments

Reaction to STM mobility mismatches: Results

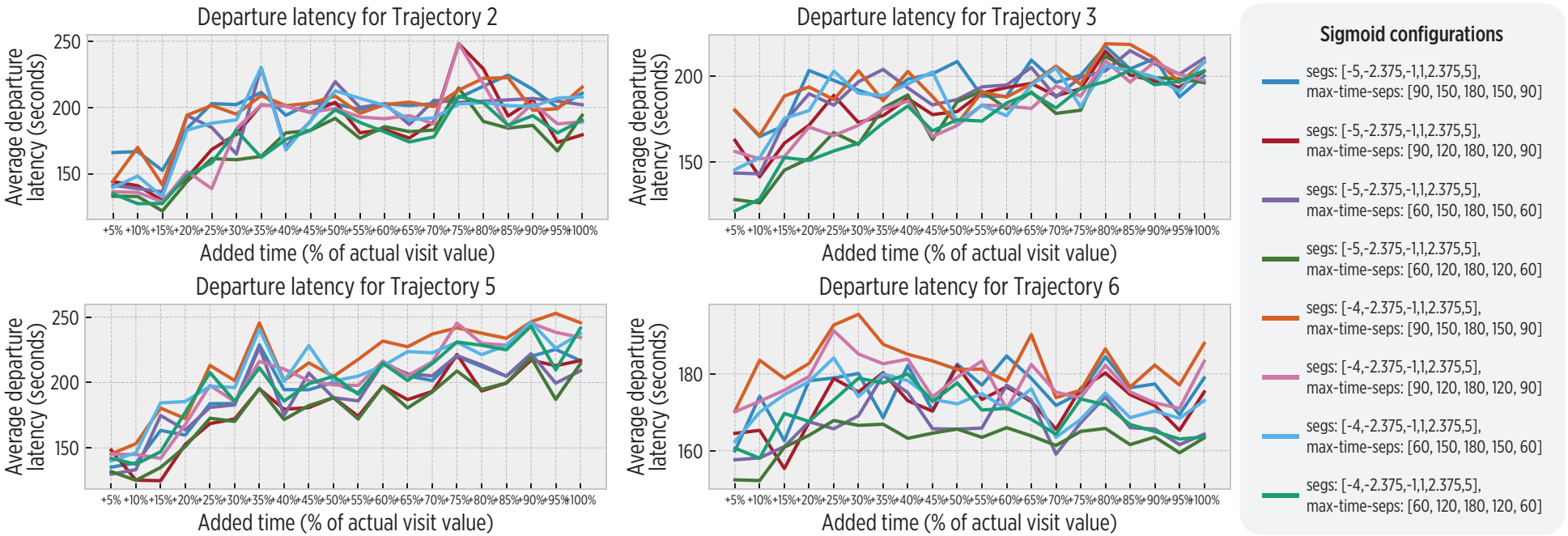

Figure: The variation of the latency values of departures detection when the STM is injured with additional time. The observed values are under the theoretical 360 seconds maximum peak.

Preliminary experiments
Holistic evaluation: Description

Description

- This experiment was aimed at evaluating the overall spatial-time accuracy performance of the system with all of its component enabled, including:
  - The continuous learning of stay points in the STM for adapting GPS sampling rate.
  - The handling of mobility mismatches.

Geofencing	**Radio distance** ($gf_{distance}$):	250 m
	Window size (gf_{ws}):	3
Cognitive Controller	**Sigmoid segments** (Θ_{domain_segs}):	$(-5, -2.375), (-2.375, -1), (-1, 1), (1, 2.375), (2.375, 5)$ $(-4, -2.375), (-2.375, -1), (-1, 1), (1, 2.375), (2.375, 5)$
	Time separations (Θ_{time_sep}):	$[90, 150, 180, 150, 90]$ seconds $[90, 120, 180, 120, 90]$ seconds $[60, 150, 180, 150, 60]$ seconds $[60, 120, 180, 120, 60]$ seconds
	On trajectory sampling:	30 seconds
	Conservative sampling:	60 seconds
Trajectories	All ground truth trajectories.	
STM	Empty	

Table: Input parameters for the holistic evaluation experiment. The *conservative* sampling refers to the late departure mismatch reaction.

Preliminary experiments

Holistic evaluation: Results

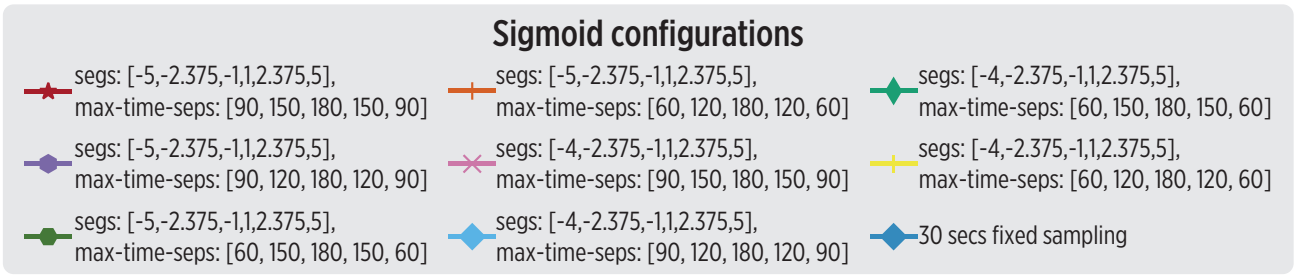

Arrival latency

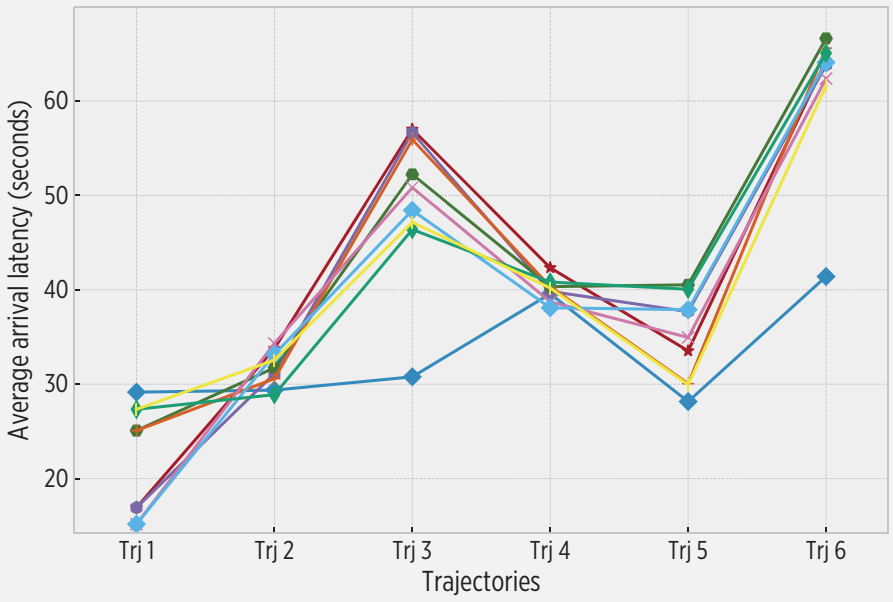

Figure: Arrival latency observed by the platform in experimental trials. The largest average value is below 65 seconds, explained by the fact that 2 location updates must be collected by the *Geofencing* module before identifying an arrival event.

Departure latency

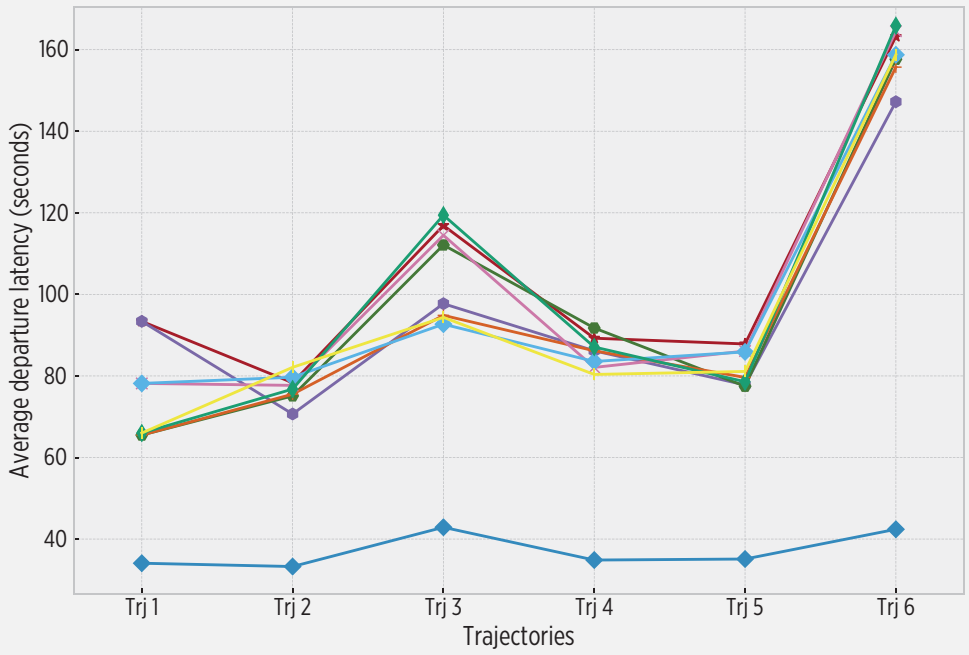

Figure: Departure latency observed by the platform across performed experimental trials. The latencies are within 65 and 165 seconds, which is aligned with the different values specified to the CC for its sigmoid-driven sampling.

Preliminary experiments

Holistic evaluation: Results

Sigmoid configurations

- segs: [-5,-2.375,-1,1,2.375,5], max-time-seps: [90, 150, 180, 150, 90]
- segs: [-5,-2.375,-1,1,2.375,5], max-time-seps: [60, 120, 180, 120, 60]
- segs: [-4,-2.375,-1,1,2.375,5], max-time-seps: [60, 150, 180, 150, 60]
- segs: [-5,-2.375,-1,1,2.375,5], max-time-seps: [90, 120, 180, 120, 90]
- segs: [-4,-2.375,-1,1,2.375,5], max-time-seps: [90, 150, 180, 150, 90]
- segs: [-4,-2.375,-1,1,2.375,5], max-time-seps: [60, 120, 180, 120, 60]
- segs: [-5,-2.375,-1,1,2.375,5], max-time-seps: [60, 150, 180, 150, 60]
- segs: [-4,-2.375,-1,1,2.375,5], max-time-seps: [90, 120, 180, 120, 90]
- 30 secs fixed sampling

Arrival distance difference

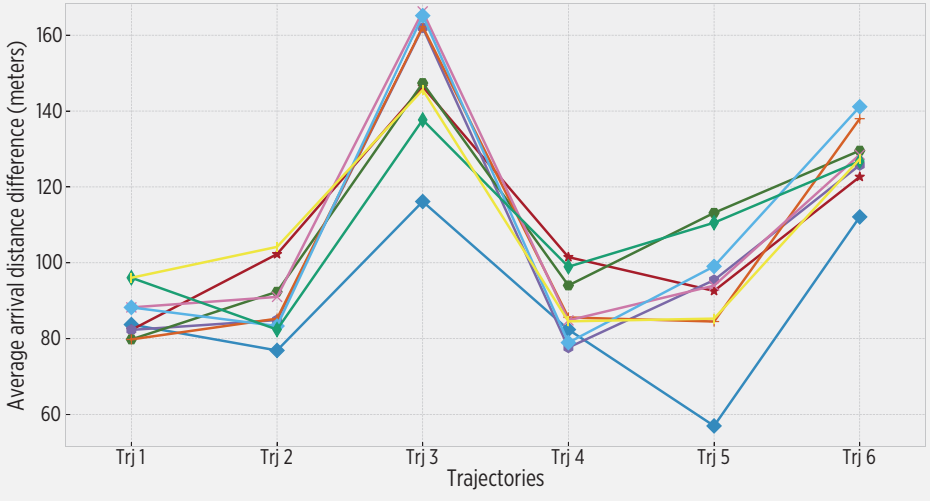

Figure: Arrival distance difference detected by the system throughout the different experimental trials. The values are shorter than for departure distance due to the decreasing speed that user describes when arriving to a stay point.

Departure distance difference

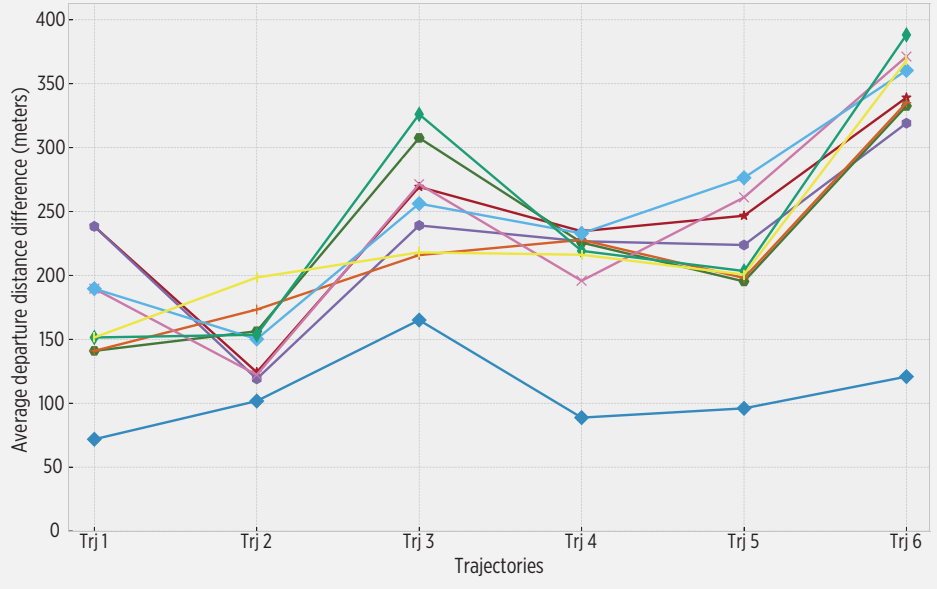

Figure: Departure distance difference detected by the system throughout the different experimental trials. The larger distance differences are caused by the high speed with which user leaves the stay points (mostly using a vehicle as transportation mode).

Preliminary experiments

Holistic evaluation: Results

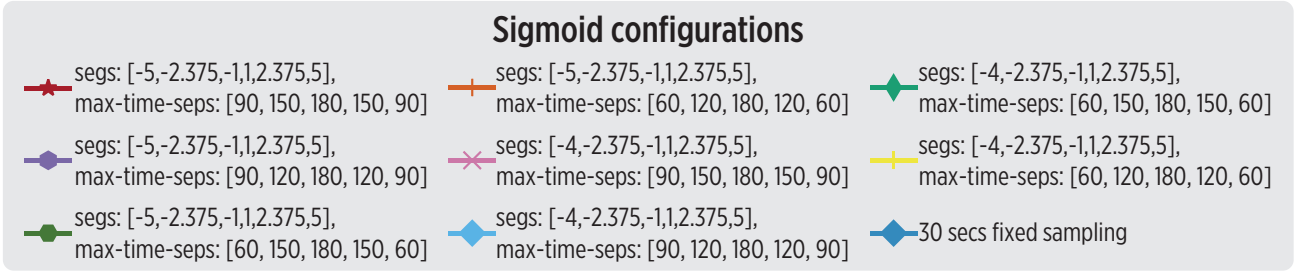

Trajectory distance difference

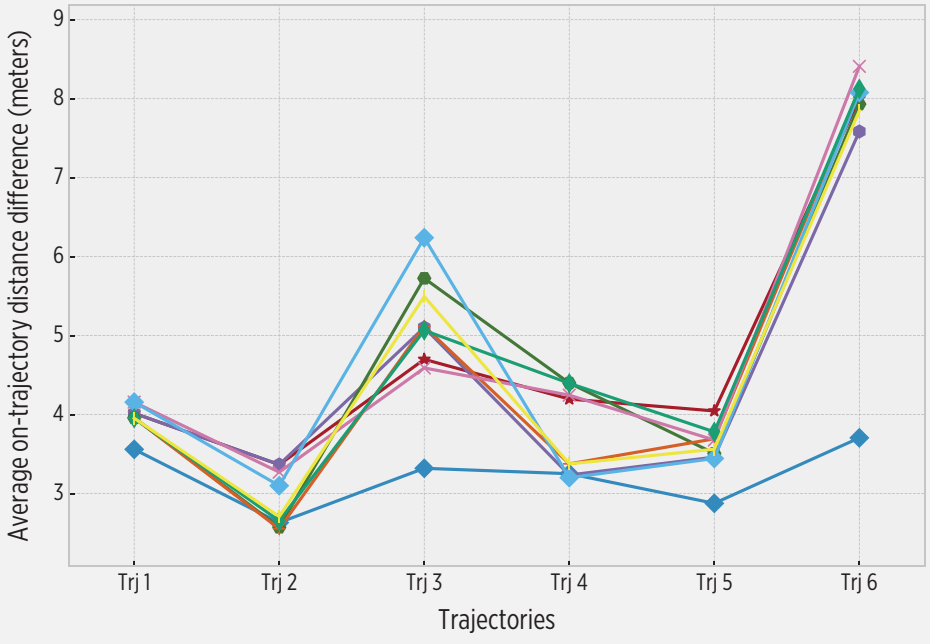

Figure: The average distance of equivalent trajectory segments during experimental trials. The values are enclosed within $2.5\,m$ and $8.5\,m$, with the 30 seconds sampling obtaining the lowest values in each trial.

Overall reduction of location update requests

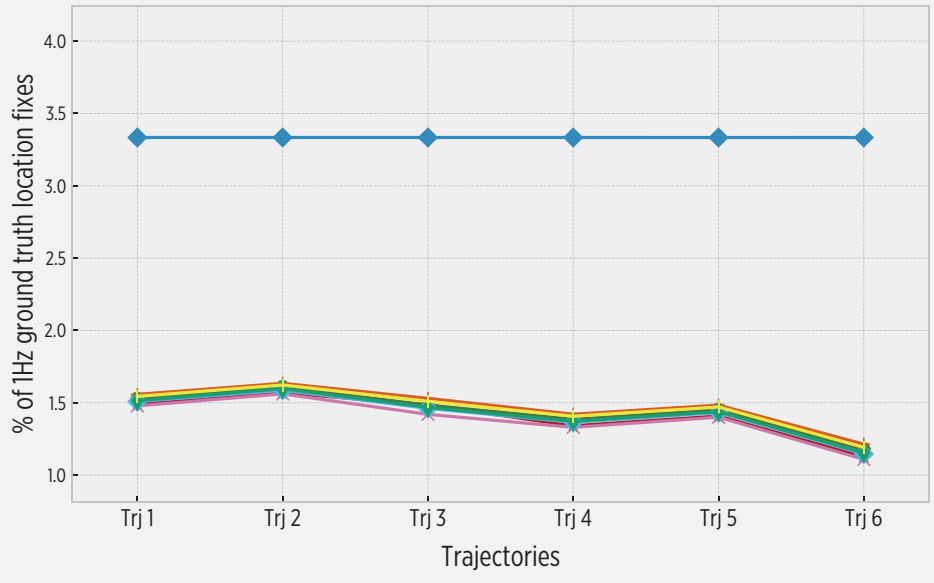

Figure: The proportion of location update requests employed by each experimental trial with respect to the corresponding 1 *Hz* ground truth trajectory. All of the parameter combinations outperform the 30 seconds sampling period, which provides a rough estimation of the energy savings that the system could achieve in on-device implementations.

Preliminary experiments

Energy saving expectations of on-device stay points detection

Description

- This experiment explored whether a smartphone could detect stay points by itself, and the energy savings of such implementation with respect of typical Mobile Cloud Computing (MCC) based solutions.

Stay Points Detector	**Time threshold** (δ_{time}):	45 *min*
	Distance threshold ($\delta_{distance}$):	500 *m*
Sampling periods:	30, 60, 90, 120, 150 seconds	

Table: Input parameters for the energy saving expectations of on-device stay points detection experiment.

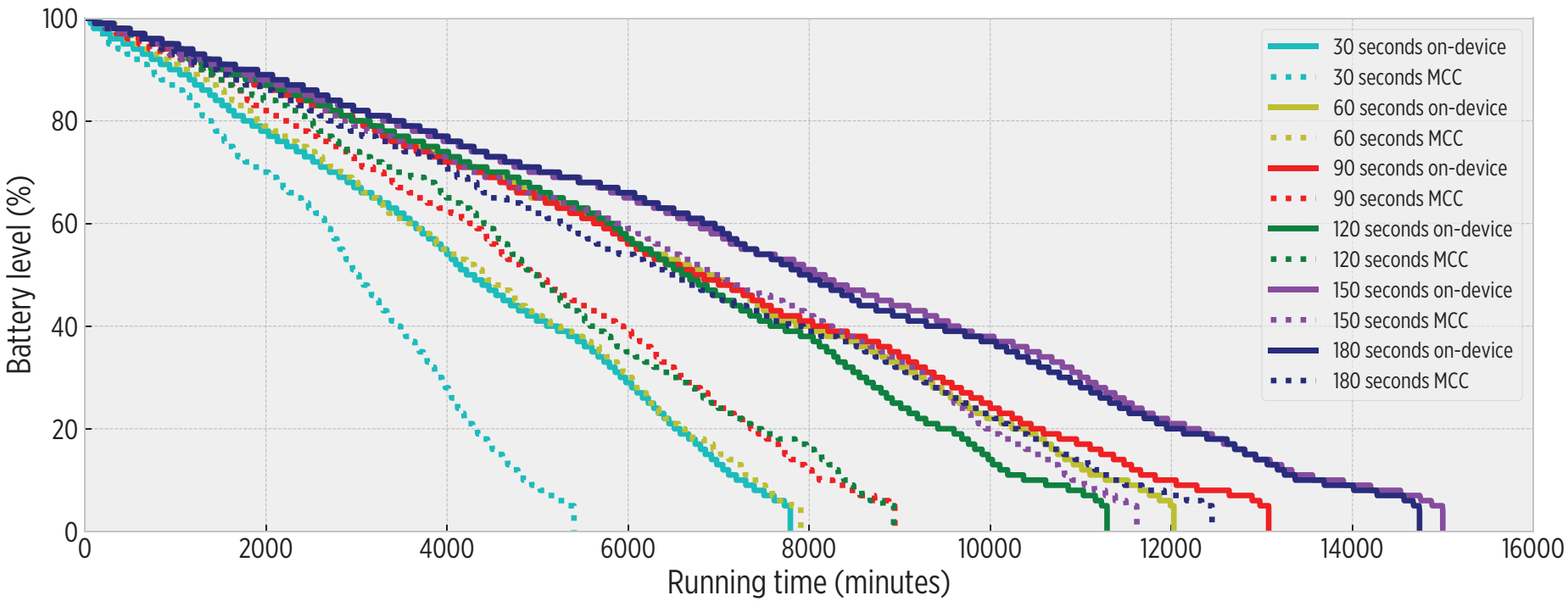

Figure: Energy performance comparison of on-device vs. MCC sample apps using different GPS sampling periods. Each of the on-device trials last longer than its corresponding remote implementation.

Preliminary experiments

Energy consumption of fixed-sampling periods: Description

Description

- This experiment evaluated the impact of sampling adaptations based on fixed sampling rates on the energy consumed by the proposed CDS.
- All system components were enabled, with the exception of the sigmoid sampling of the CC.
- The CC followed fixed sampling periods depending on the current mobility state recognized by the system.
- The experiment also demonstrated the mobility awareness that the system provides to the smartphone (STM).

Stay Points Detector	**Time threshold** (δ_{time}):	45 *min*
	Distance threshold ($\delta_{distance}$):	500 *m*
Geofencing	**Radio distance** ($gf_{distance}$):	250 *m*
	Window size (gf_{ws}):	3
HAR module	**Individual window length**:	5 seconds
	Meta-window size (HAR_{mws}):	5
Cognitive Controller	**Smartphone 1**:	On trajectory sampling periods: 30 seconds On stay point sampling period: 30 seconds
	Smartphone 2:	On trajectory sampling period: 30 seconds On stay point sampling period: one in the set $\{60, 90, 120, 150, 180\}$ seconds

Table: Input parameters for the energy consumption of fixed-sampling periods experiment.

Preliminary experiments

Energy consumption of fixed-sampling periods: Results

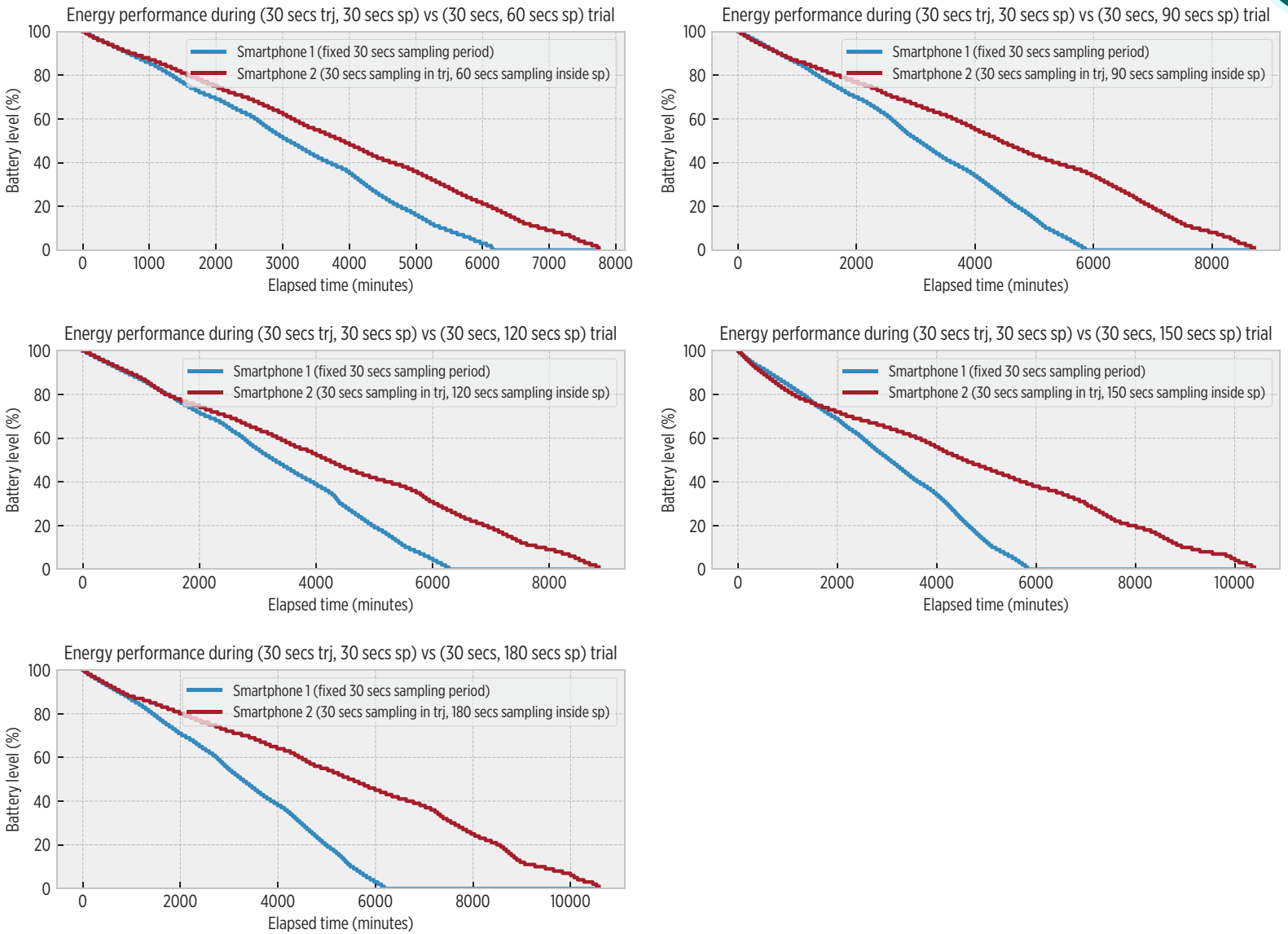

Figure: Energy performance of a fixed 30 seconds sampling versus a basic sampling adaptation consisting in a 30 seconds sampling in trajectory mode and a slower sampling rate during stay point mode. The separation between the lines in each plot starts after the system learns the stay points with the largest weight in user mobility (home and work places).

Preliminary experiments

Energy consumption of fixed-sampling periods: Results

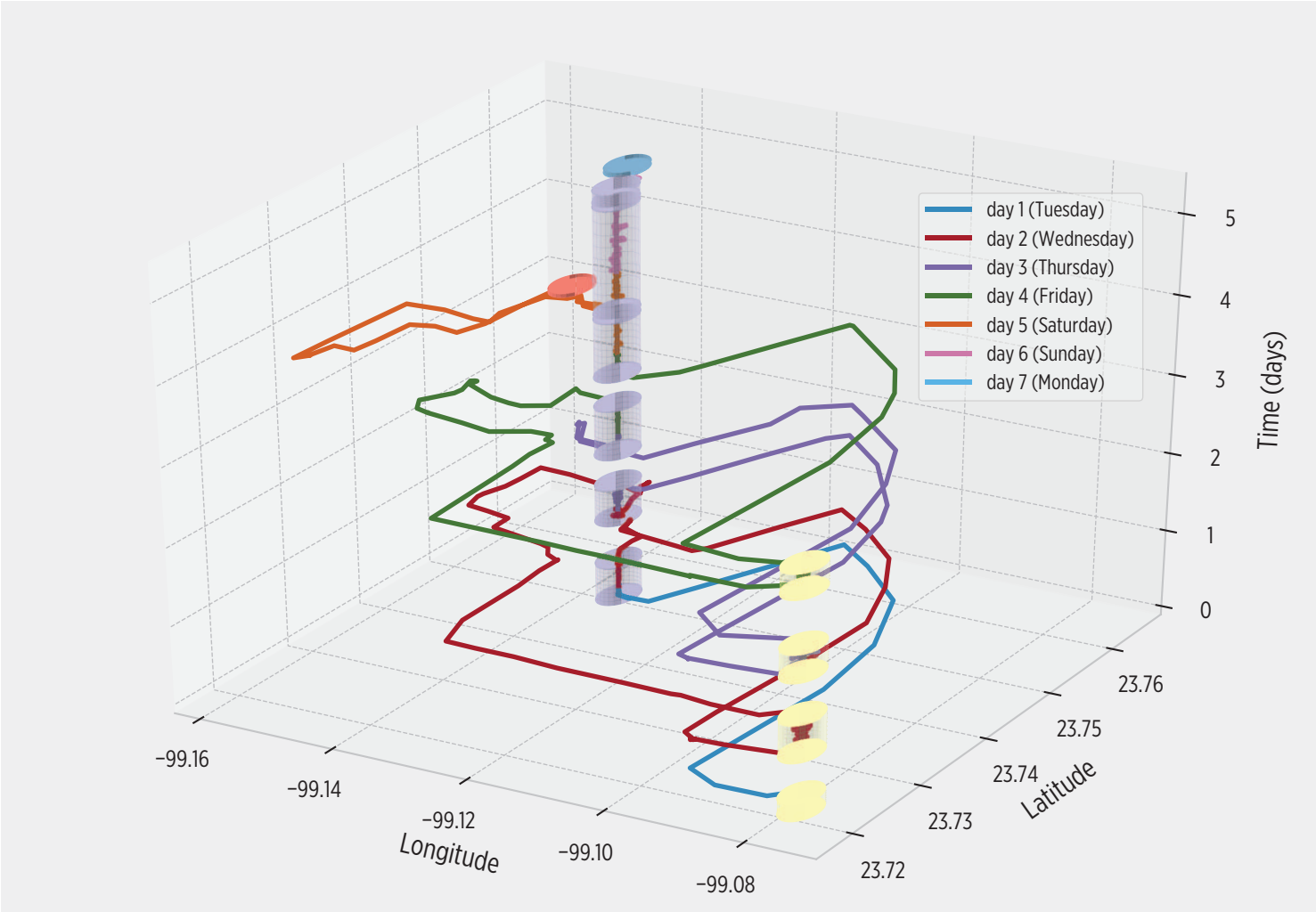

Figure: The information autonomously learned by the STM during the trial corresponding to the 30 seconds in trajectory and 60 seconds in stay point sampling scheme. The height of cylinders corresponds with the stay time during each stay point visit.

Preliminary experiments

Comparison with other solutions

Work	Purpose	Mobility type	Involved sensors	Trajectory tracking	Place learning
SenseLess	Location tracking	Walking, static	Accelerometer, GPS	Yes	No
SmartDC	Place tracking	Not specified	Cellular id, Wi-Fi, GPS	No	Yes
Proposed system	Location and place tracking	Static, walking, biking, vehicle	Accelerometer, GPS	Yes	Yes

Table: Features comparison of proposed system and representative existing solutions.

Future work

Pending tasks

#	Activity	2017 Aug	Sep	Oct	Nov	Dec	2018 Jan	Feb	Mar	Apr	May	Jun	Jul	Aug
	Solution refinement activities													
1	Incorporation of the HAR module in the CC	■	■											
2	Incorporation of the accuracy requirement in the CC		■	■	■									
	On-device implementation													
3	Implementation of sigmoid-driven sampling				■									
4	Watchdog mechanisms for *Geofencing* and *Sampling Decision Maker* modules				■	■								
5	Refinement of the list of candidate stay points employed by the *Geofencing* module				■	■	■							
	Experimentation													
6	Experiments with larger and heterogeneous mobility						■	■	■					
7	Completion of evaluation framework					■	■	■						
8	Comparison with other solutions									■	■			
	Research work activities													
9	Thesis writing-review								■	■	■	■	■	
10	Thesis defense													■

Table: Schedule of pending activities of the research work for the last year of the doctoral program.

Future work

Incorporation of the HAR module in the CC

Incorporation of the HAR module in the CC

- For aiding the detection of departures in stay point mode:
  - The center segments of the generated sigmoid sampling could employ HAR instead of GPS location updates. GPS can confirm the motion detection.
  - It could avoid the fixed *conservative sampling* of the late departure mismatch reaction.
- For adaptive GPS sampling during trajectory mode:
  - A consecutive static outcome from the HAR module could reduce GPS sampling rate, otherwise it could be incremented according to detected transportation mode.

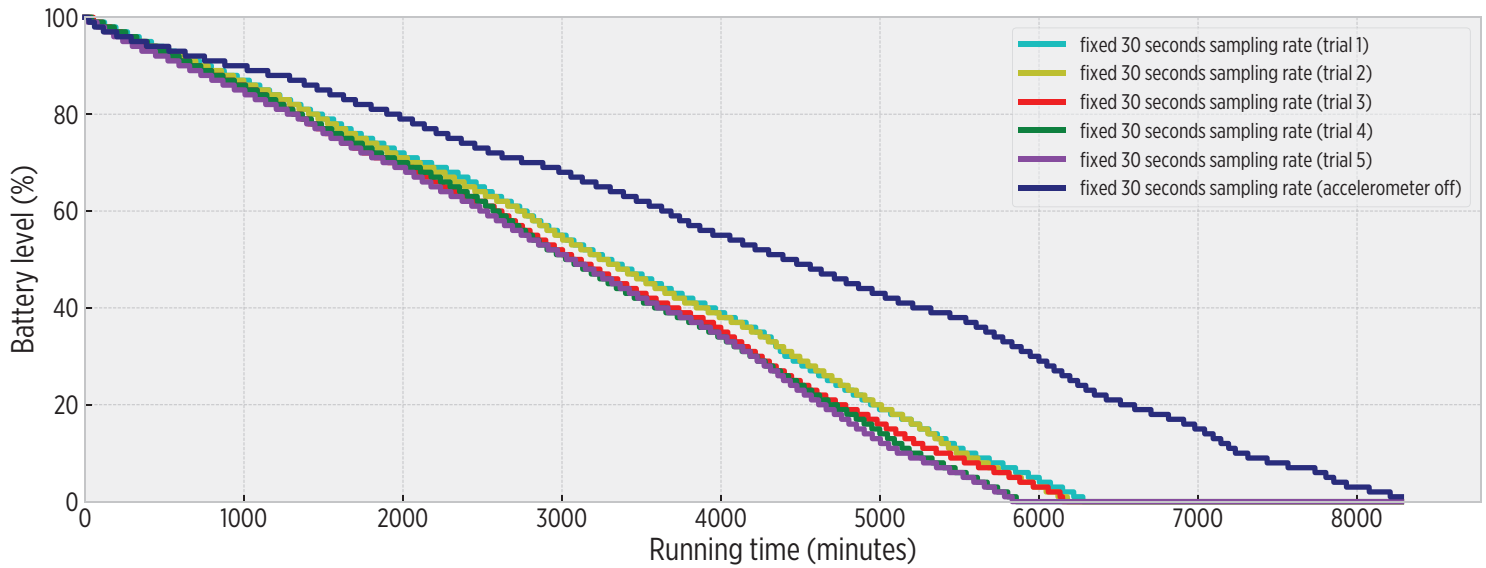

Figure: Energy consumption performance of the fixed 30 seconds GPS sampling trials with HAR module enabled, versus a fixed 30 seconds GPS sampling trial with HAR disabled. The battery lasts 1.5 days longer when HAR module is not enabled.

Conclusions

Conclusions

- The experiments demonstrate the system's ability to identify the coarse-grain mobility events for building the STM. A first approximation shows that:
  - Centroid distance between ground truth and observed stay points is at most $22.5m$.
  - All stay points are detected, the arrival and departure latencies are within the active sampling rate.
  - The length of the visits missed by the *Geofencing* are short, no longer than 4 minutes.
- The STM information has proved its usefulness for the CC to reduce energy consumption with a minor impact on spatial-time accuracy:
  - The latencies and spatial differences at arrival and departure events are within the expected values.
  - Only 33 – 49 % of the location updates of a fixed $30s$ sampling rate are employed in simulations.
  - On-device trials show a battery life increase of $26 — 76h$, with respect of a fixed $30s$ sampling rate.
- The hypothesis is demonstrated as shown by the implementation of the CDS and the associated experimentation.
- The EDS approach eases the design and implementation of the system, as it suits the characteristics of mobile platforms. Nevertheless, experimentation is needed to assess its energy performance.
- The developed middleware isolates sensors and power management complexity for long-term LBSs and MBSs.

Conclusions

Doctoral program requirements

- All the subject courses suggested by the admission committee were attended during the first year.
- A recommendation for refinement of the state of the art has been fulfilled.
- Such refinement and other advances performed on the research work has been submitted for publications (two journal articles [12, 13]).

Thank you for your attention!

Consider again that dot [Earth]. That's here. That's home. That's us.

Carl Sagan

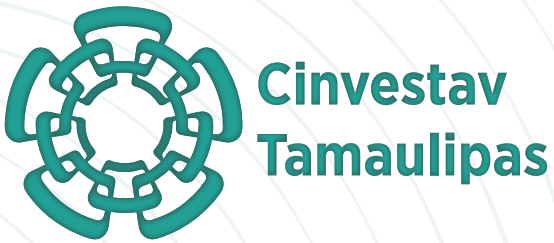

References I

[1] Guanling Chen and David Kotz.
A Survey of Context-Aware Mobile Computing Research.
Technical report, 2000.

[2] Mikkel Kjaergaard.
Location-based services on mobile phones: Minimizing power consumption.
IEEE Pervasive Computing, 11:67–73, 2012.

[3] Xiao Ma, Yong Cui, and Ivan Stojmenovic.
Energy efficiency on location based applications in mobile cloud computing: A survey.
In *Procedia Computer Science*, volume 10, pages 577–584, 2012.

[4] Eric C. Evarts.
Lithium batteries: To the limits of lithium.
Nature, 526(7575):S93–S95, oct 2015.

[5] Opher Etzion and Peter Niblett.
Event Processing in Action.
Number ISBN: 9781935182214. Manning Publications, 2010.

[6] Ted Faison.
Event-based programming: Taking events to the limit.
Apress, Berkely, CA, USA, 1st edition, 2006.

[7] Reza Rawassizadeh, Martin Tomitsch, Manouchehr Nourizadeh, Elaheh Momeni, Aaron Peery, Liudmila Ulanova, and Michael Pazzani.
Energy-Efficient Integration of Continuous Context Sensing and Prediction into Smartwatches.
Sensors, 15(9):22616–22645, sep 2015.

[8] Chen-Yi Lee, Kelvin Yi-Tse Lai, and Shu-Yu Hsu.
A Sensor-Fusion Solution for Mobile Health-Care Applications.
In Youn-Long Lin, Chong-Min Kyung, Hiroto Yasuura, and Yongpan Liu, editors, *Smart Sensors and Systems*, pages 387–397. Springer International Publishing, Cham, 2015.

[9] Cormac Duffy, Utz Roedig, John Herbert, and Cormac Sreenan.
An Experimental Comparison of Event Driven and Multi-Threaded Sensor Node Operating Systems.
In *Fifth Annual IEEE International Conference on Pervasive Computing and Communications Workshops (PerComW'07)*, volume 3, pages 267–271. IEEE, mar 2007.

References II

[10] Laura Alessandretti, Piotr Sapiezynski, Sune Lehmann, and Andrea Baronchelli.
Multi-scale spatio-temporal analysis of human mobility.
PLOS ONE, 12(2):e0171686, feb 2017.

[11] Xiang-Wen Wang, Xiao-Pu Han, and Bing-Hong Wang.
Correlations and Scaling Laws in Human Mobility.
PLoS ONE, 9(1):e84954, jan 2014.

[12] Rafael Pérez-Torres, César Torres-Huitzil, and Hiram Galeana-Zapién.
Power management techniques in smartphone-based mobility sensing systems: A survey.
Pervasive and Mobile Computing, pages 1–21, feb 2016.

[13] Rafael Perez-Torres, Cesar Torres-Huitzil, and Hiram Galeana-Zapien.
Full on-device stay points detection in smartphones for location-based mobile applications.
Sensors (Switzerland), 16(10), 2016.